High-Dimensional Entanglement Generation with Linear Optics

Niv Bharos

Master Thesis
Delft University of Technology

High-Dimensional Entanglement Generation with Linear Optics

by

Niv Bharos

to obtain the degree of Master of Science
at the Delft University of Technology,
to be defended publicly on Wednesday May 17, 2023 at 09:30 AM.

Student Number:	4437233	
Project Duration:	September 5, 2022 – May 17, 2023	
Thesis Committee:	Prof. dr. ir. R. Hanson	QuTech
	Dr. M. Blauuboer	TU Delft
	Dr. J. Borregaard	QuTech, supervisor
	Dr. L. Markovich	Leiden University, supervisor

TU Delft

Preface

You are reading the thesis 'High-Dimensional Entanglement Generation with Linear Optics' in which two protocols are proposed to generate N-dimensional entanglement between bipartite systems. This research was carried out in the group of Johannes Borregaard as part of the master's program Applied Physics with a specialization in Quantum Devices and Quantum Computing at Delft University of Technology.

About a year ago, Johannes outlined two possible projects to me. I am sure the first project was very interesting but I cannot remember it sadly. What I do recall is that Johannes described the second project as 'high risk, high reward'. Of course now I was sold. Not because of the high reward (actually, when can I expect that?) but because I stumbled upon a similar problem a few weeks before the meeting. Then I had no time to think about it because there were courses to follow, so I was very excited with the chance to work on it for my thesis.

I want to thank Johannes for being so invested with long discussions every week and for all of his incredibly smart ideas. It has been a very nice introduction to research under his guidance and that he was always open to my ideas meant a lot to me. Many ideas presented in this thesis were his. After the build-up of the past months I am very curious to see where he ends up but they will be lucky to have him on their side! I was also supervised by Liubov Markovich who was always open to talking about the project and sharing her experiences in academia. Thanks for listening to my ideas and for having many fun discussions about (quantum) physics, even at a Christmas dinner or consortium.

I would like to thank everyone in the group of Johannes for the fun times during social activities and the interesting discussions during the group meetings. My fellow students in the master's office made daily life all the more fun. As a theorist, you are definitely a minority in this office and the stories of the experimental thesis students were foreign yet very fascinating to hear. One thing that we have in common though is that we enjoy long and frequent coffee breaks. Thank you to Zarije, Sezer, Douwe, Thomas, Elvis, Adria, Gerben, Colin, Kenji, Odiel, Dani, Wastu and Caroline. Luckily, there are amazing theorists to be found at QuTech as well. I look forward to doing more physics and of course the occasional ~~vacation~~ summer school with Hemant, Janice and Xiaoyu.

Thanks to my family and friends for their unconditional love and support. In special I want to thank Andreas. I am well aware that there is a trade-off between seeing each other at bar evenings versus studying together in the evenings and for example, discussing the planetary orbitals when Mercury is in retrograde. I have high hopes that we can catch up over the summer! Lastly, special thanks to Daniël for sharing his wisdom about the PhD life and for always encouraging me.

Hope you enjoy reading this thesis.

Niv Bharos
Delft, May 2023

Summary

For many quantum applications we require high-fidelity entanglement between multiple pairs of solid state qubits at a distance. To achieve a high fidelity, we have to minimize the time during which the generated qubits need to stay coherent. Entanglement protocols often used in practice only generate one qubit at the same time. To generate multiple entangled pairs, the protocol is repeated. However during the time it takes for all pairs to be generated, the memory qubits will dephase. The required coherence time increases with the inverse transmission probability of the photons, which decreases exponentially with distance. This thesis is concerned with entanglement generation protocols that herald multiple entangled pairs simultaneously and in general herald N-dimensional entangled bipartite states. The main advantage of using more than 2 dimensions is that the qudits only dephase during the time in which the protocol executes. With simulations we show that the fidelity of the entangled pairs created with our protocols is higher than the fidelity of pairs created by protocols that heralds one entangled pair for distances $L \geq 10$ km. We also show a polynomial relation between the total success probability of the tailored protocol with dimension, which is an exponential improvement with respect to previous works. We first give background information in Chapter 2 and discuss existing high-dimensional protocols in Chapter 3. We propose the all-input modes entanglement protocol in Chapter 4 and a novel protocol in Chapter 5: the tailored protocol.

Contents

1 Introduction

Entanglement is a peculiar phenomenon in the realm of quantum mechanics that Einstein described as *spooky action at a distance*. It is peculiar because it does not align with our classical intuitions. This is the setting: there are two parties that we usually call Alice and Bob and they are far apart. They both have a fair coin that they toss once. In the classical case Alice may get heads and when Bob tosses his coin, he still has a probability of $\frac{1}{2}$ to get heads and probability $\frac{1}{2}$ to get tails. We call the events of tossing two coins uncorrelated. The coins can in reality never be qubits, but let us pretend that the coins are qubits and that they are entangled in the following way:

$$\frac{1}{\sqrt{2}}\left(|H_A H_B\rangle + |T_A T_B\rangle\right) \quad . \tag{1.1}$$

Here H represents heads, T represents tails and the subscript A and B indicate the coin of Alice or Bob. If Alice tosses her coin now and gets heads, Bob will get heads for sure as well. Similarly, if Alice gets tails, Bob gets tails. This example illustrates that correlations between quantum systems can be higher than we get in the classical setting.

The stronger correlations of entangled quantum systems play an important role in quantum technology. One example is that by entangling remote quantum nodes, we can create a secure quantum communication channel. If an eavesdropper tries to intercept the message, the parties trying to communicate can detect this as a change in the correlation of their states. Motivated by algorithms like these, many current experimental and theoretical efforts go towards entangling remote nodes [8]. The aim is to entangle many quantum nodes in the (hopefully not-so-far) future, thereby creating a quantum network. Aside from secure communication [18], quantum networks will allow us to execute some algorithms faster [28] and even increase the resolution of instruments like telescopes [22]. In this thesis we take a closer look at generating entanglement with a high rate from a theoretical perspective.

Recent research has demonstrated entanglement generation between remote nodes with various physical platforms: between rare-earth doped solids [31], quantum dots [46] and NV centers [40]. These schemes rely on entanglement swapping: first, the nodes are entangled with photons. By interfering the photons at a middle station, entanglement is probabilistically heralded. Here, one Bell pair is generated in one successful run of the protocol. By executing the same protocol multiple times in parallel (multiplexing), we can generate multiple pairs at the same time. However, dephasing still lowers the average fidelity of the generated entangled pairs. To see this, let's consider an example where we want to entangle two qubits.

1.1. Motivating Example

Alice and Bob are far apart and they want to entangle two qubits to use in a quantum algorithm to create a secret key of two bits. They want the quality of entanglement, the so-called fidelity, to be high such that they are very likely to get the same secret key. To generate entanglement they use an entanglement protocol that generates one entangled qubit pair in one successful run of the entanglement protocol and succeeds with a probability p. This probability decreases exponentially as the distance between Alice and Bob increases. If Alice and Bob execute the entanglement protocol twice at the same time, the probability to generate all pairs at the same time is small for large distances. We give a visualization of two possible outcomes in Figure 1.1. In (a_1) and (b_1), Alice and Bob execute the protocol for both qubits in parallel. In (a_2) we show the case where both protocols immediately succeed. However if we are less lucky, one entangled pair is generated but the protocol fails for the second pair (b_2). The second qubits of Alice and Bob have to execute the protocol again (b_3). Now the protocol succeeds at best in this second try (b_4).

The problem is that the quality of the qubits decreases over time and this lowers the average fidelity of the generated entangled pairs. In case (a), the qubits have to wait during the time it takes to execute the protocol once. In case (b), the qubit that is entangled in the first try has to wait until the other pair is generated. Since the probability of success is low for large distances, this can take a while.

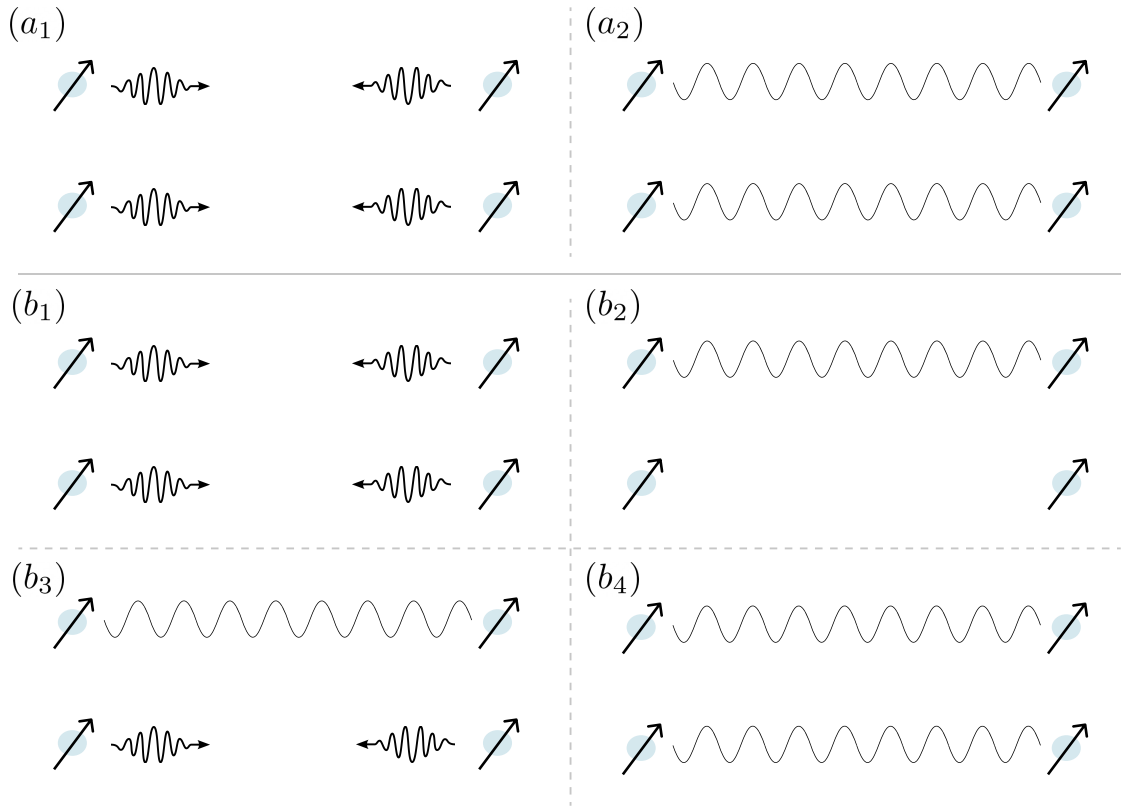

Figure 1.1: Alice and Bob want to generate two entangled pairs with an entanglement protocol. The protocols is executed simultaneously for both pairs (a_1) and (b_1). (a_2) is the case where the protocol succeeds twice at the same time. (b_2) is the case where one attempt succeeds and the other fails. The protocol is executed again for qubits that are not entangled (b_3) and (b_4) is the case where the attempt succeeds during the second round.

Moreover, there are even worse cases where the first entangled pair has to wait for a longer time. Also, if Alice and Bob want to entangle more qubits the waiting time increases even more. We can

avoid this long waiting time by generating multiple entangled pairs in one successful run. By heralding multiple entangled pairs simultaneously, the waiting time of all qubits is limited to the time of one execution of the protocol. Thus the average fidelity is higher than when the entangled pairs are generated sequentially. Moreover, we aim to generate a general form of entanglement: high-dimensional entanglement. Alice and Bob want to entangle N energy levels where the number of energy levels does not necessarily correspond to an integer number of qubits d: $N \neq 2^d$.

1.2. Research Goals

Recent work by Yunzhe et al. [50] proposes to create multiple entangled pairs in one successful run of the protocol by using photonic qudits: a photon encoded in more dimensions than two. However the implementation outlined by Yunzhe et al. requires multiple emitters strongly coupled to optical resonators and fast optical switching, which makes it difficult to implement in practice. In this thesis we want to generate high-dimensional entanglement while lowering the demands on the physical systems: we want to perform a Bell state measurement (BSM) on the photonic qudits of Alice and Bob with linear optical elements. Therefore our main research question is:

"How can we use linear optical elements and time-bin encoded photonic qudits to herald high-dimensional entanglement between remote qudits?"

1.3. Contributions

Previous works by Luo et al. [32] and Zhang et al. [48] have proposed a Bell state measurement at the middle station that relies on implementing an N-dimensional quantum Fourier transform in order to perform quantum teleportation in N dimensions. Luo et al. demonstrate experimental quantum teleportation of a three-dimensional state encoded in a photon. However their implementation requires N^2 spatial modes and photon detectors. In our first protocol, the all-input modes protocol, we propose an adaptation of the protocol of Luo et al. where we use photonic qudits encoded in time-bins. We only need N spatial modes and photon detectors and by using a time-bin encoding the photons are robust to bit flips during transmission and no additional [10].

Additionally, the success probability of the protocol of Luo et al. does not scale well with dimension. The Bell state measurement is upper bounded by $p_{\text{succ}} = \frac{N!}{N^N}$. Zhang et al. improve this success probability to a polynomial scaling in their protocol that we call the permutation protocol from now on. However, their implementation requires another Bell state measurement which lowers the total success probability to an even worse scaling than p_{succ}. Thus, an efficient protocol of the high-dimensional Bell state measurement is missing in current research.

We propose a new protocol for high-dimensional entanglement generation that achieves a success probability $p_{\text{succ}} = \frac{2}{N^2}$ for all even dimensions. This is an exponential improvement compared to existing protocols and we show that this success probability can be achieved for every even dimension. Also, the initial states necessary for our protocol are entangled, but they are not EPR pairs as Zhang et al. [48] require. We propose a deterministic way to create the initial states necessary for our protocol which is the main advantage over the permutation protocol since we do not need an additional Bell state measurement that would lower the total success probability. To summarize, our main contributions are:

1. An adaptation of the protocol of Luo et al. that uses time-bins instead of spatial modes and thus lowers the number of required hardware elements with a square root and is more robust to bit flips.
2. A novel tailored protocol for high-dimensional entanglement generation in even dimensions that outperforms the state of the art on success probability and hardware requirements.

3. With simulations we show that for distances approximately $L \geq 10$ km the average fidelities of high-dimensional entanglement protocols perform better than the average fidelities of existing protocols.

1.4. Outline

The rest of this thesis is structured as follows. We start with background information in chapter 2 and evaluate previous works on high-dimensional Bell state measurements. In chapter 4 we describe our first high-dimensional entanglement protocol that uses an equal superposition as input to the interferometer: the all-input modes protocol. In chapter 5 we propose our second protocol with a tailored input state: the tailored protocol. We compare our protocols to each other and to existing entanglement protocols in chapter 6 and conclude in chapter 7.

2

Background Information

In this chapter we start with the fundamentals of quantum information: we describe concepts such as qudits and entanglement. This discussion is largely based on chapters from Nielsen and Chuang [36]. Since 2000 quantum computation with photons has been widely researched. We aim to give a background for quantum computation with linear optical elements. We discuss a protocol that uses entanglement as a resource and linear optical elements: quantum teleportation. Finally we consider optical switches, a non-linear optical element that we encounter in Section 5.6.

2.1. From Qubits to Qudits

When we talk about quantum technology, we usually think about quantum circuits with qubits being the main unit of information. This qubit is fundamentally different from the classical bit: the classical bit can exist in the state 0 or 1, but not both at the same time. Qubits can exist in a superposition of both states simultaneously. This property is often used in some quantum algorithms to apply a function to all possible input states at the same time, for example in Shor's algorithm to factorize large numbers [44]. The wave function describes the state of a quantum system with the standard notation for quantum states: the Dirac notation '$|\,\rangle$'.

$$|\psi\rangle = \alpha\,|0\rangle + \beta\,|1\rangle \qquad \alpha,\beta \in \mathbb{C} \wedge |\alpha|^2 + |\beta|^2 = 1 \ . \tag{2.1}$$

Here, $|0\rangle = \begin{bmatrix}1\\0\end{bmatrix}$ and $|1\rangle = \begin{bmatrix}0\\1\end{bmatrix}$. We rewrite Eq. (2.1) to:

$$|\psi\rangle = e^{i\delta}\left(\cos\frac{\beta}{2}\,|0\rangle + e^{i\phi}\sin\frac{\beta}{2}\,|1\rangle\right) \qquad \phi \in [0,2\pi],\ \beta \in [0,\pi] \ . \tag{2.2}$$

In this representation, the state of a single qubit can be visualized on the Bloch sphere defined by the phases β and ϕ. The global phase factor δ is always neglected since it does not have any physical relevance. We give a visualization of the state corresponding to Eq. (2.2) on the Bloch sphere in Figure 2.1.

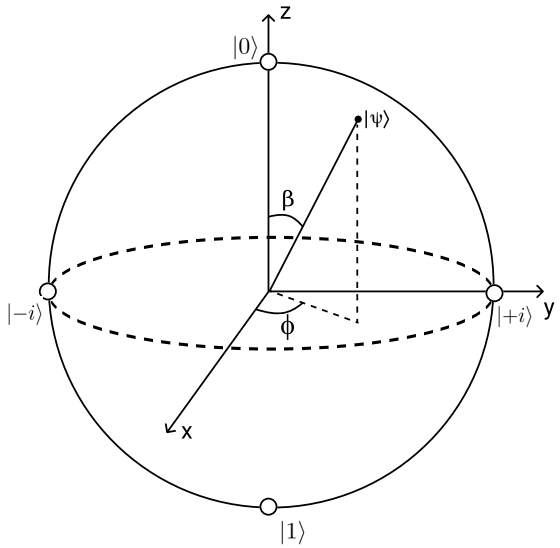

Figure 2.1: Representation of the state of a qubit on the Bloch sphere.

2.1.1. Photonic Degrees of Freedom

Quantum information can be stored in various physical systems, for example in the energy levels of Rubidium atoms [43], the energy levels of a defect in diamond [25] or in a degree of freedom of photons [19]. Entanglement generation protocols use photons to generate entanglement between remote nodes since photons are the ideal carriers of quantum information over large distances: they travel with the speed of light and have almost no interactions with the environment. We consider some examples of photonic degrees of freedom:

1. **Polarization.** Photons can have a horizontal $|H\rangle$ or vertical $|V\rangle$ linear polarization and these states are orthogonal to each other. A general wavefunction looks like:

$$|\psi\rangle = \alpha\,|H\rangle + \beta\,|V\rangle \qquad \alpha,\beta \in \mathbb{C} \wedge |\alpha|^2 + |\beta|^2 = 1 \ . \tag{2.3}$$

2. **Time-bins.** There are multiple ways of encoding quantum information in time-bins. The single rail encoding uses the absence $|\mathrm{vac}\rangle$ or presence $|0\rangle$ of a photon in one time-bin that we call 0 here.

$$|\psi\rangle = \alpha\,|\mathrm{vac}\rangle + \beta\,|0\rangle \ . \tag{2.4}$$

The dual rail encoding uses two time-bins, for example 0 and 1. A general state looks like:

$$|\psi\rangle = \alpha \cdot \hat{a}_0^\dagger |\mathrm{vac}\rangle_0 |\mathrm{vac}\rangle_1 + \beta \cdot \hat{a}_1^\dagger |\mathrm{vac}\rangle_0 |\mathrm{vac}\rangle_1 \ . \tag{2.5}$$

Here, $\hat{a}_i^\dagger$ is the creation operator of a photon in time-bin i. Usually the more convenient notation is used and the vacuum is omitted. We write down time-bin i of the photon as $|i\rangle$:

$$|\psi\rangle = \alpha\,|0\rangle + \beta\,|1\rangle \ . \tag{2.6}$$

Now $|0\rangle$ indicates a photon in time-bin 0 and $|1\rangle$ a photon in time-bin 1. We use the time-bin encoding often in this thesis and in Section 2.3.1 we discuss how we can encode any quantum state in time-bins by using linear optical elements.

3. **Frequency.** Quantum information can also be stored in two discrete frequencies of a photon.
4. **Path degree of freedom (spatial modes).** By using two optical fibers we can encode a photonic qubit. The state $|0\rangle$ can correspond to a photon in fiber 0 and $|1\rangle$ to a photon in fiber 1.

There are more degrees of freedom of photons that can be used and combinations of photonic degrees of freedom are also used. For example in Section 3.3.3 we discuss a paper that uses both the spatial mode encoding of photons and their polarization.

Most quantum systems have access to more than two distinguishable quantum states and by using these levels, a qudit is created. A qudit is the generalization of a qubit: it has N orthogonal states with $N > 2$. Examples include the *qutrit*, a three-level system, or the lesser known *ququart*, a four-level system. Similar to qubits, qudits can be in a superposition of quantum states. An example of a qudit state in four dimensions is:

$$\begin{aligned} &|\psi\rangle = \alpha_0 |0\rangle + \alpha_1 |1\rangle + \alpha_2 |2\rangle + \alpha_3 |3\rangle \\ &\alpha_0, \alpha_1, \alpha_2, \alpha_3 \in \mathbb{C} \ \wedge \ |\alpha_0|^2 + |\alpha_1|^2 + |\alpha_2|^2 + |\alpha_3|^2 = 1 \ . \end{aligned} \tag{2.7}$$

Here, the physical realization of quantum state $|i\rangle$ could be the occupation of time-bin i by a photon or a photon occupying spatial mode i. The general form of a qudit with N levels is:

$$\begin{aligned} &|\psi\rangle = \sum_{k=0}^{N-1} \alpha_k |k\rangle \\ &\alpha_k \in \mathbb{C} \ \wedge \ \sum_{k=0}^{N-1} |\alpha_k|^2 = 1 \ . \end{aligned} \tag{2.8}$$

Just like photonic qubits, photonic qudits can be encoded in many degrees of freedom. In this thesis, we only encounter qudits encoded in time-bins and spatial modes. We aim to use qudits to herald a high-dimensional entangled state, but qudits have been considered for other applications: for example for noise resistance in quantum key distribution schemes [5][14] and as we discuss in Section 3.3.3 for high-dimensional quantum teleportation.

2.1.2. Photon Loss over Optical Fibers

When photons are transmitted over an optical fiber, the probability of successfully transmitting the photon decreases exponentially as a function of distance:

$$p_T \sim e^{-L/L_{\text{att}}} \ . \tag{2.9}$$

Here L_{att} is the attenuation length of the fiber. We assume this coefficient to be $L_{\text{att}} = 20$ km, which corresponds to light traveling through an optical fiber in the telecom range (the range of frequencies for which the photon loss is minimized). Thus, the probability of successfully transmitting a photon decreases to $\frac{1}{e}$ if the photon travels over a distance $L = 20$ km.

2.2. Entanglement

Aside from superpositions, an important difference between quantum physics and the classical description of the world is entanglement. Alice and Bob each have a qubit. Their quantum state is entangled if the joint bipartite state $|\psi\rangle_{AB}$ cannot be written as a product state of the local particles $|\psi\rangle_A$ and $|\psi\rangle_B$:

$$|\psi\rangle_{AB} \neq |\psi\rangle_A \otimes |\psi\rangle_B \ . \tag{2.10}$$

In the two-level quantum state, the four maximally entangled states that form a basis are the Bell states:

$$\begin{aligned} |\Phi^+\rangle &= \frac{1}{\sqrt{2}}\left(|0\rangle_A|0\rangle_B + |1\rangle_A|1\rangle_B\right) \qquad |\psi^+\rangle = \frac{1}{\sqrt{2}}\left(|0\rangle_A|1\rangle_B + |1\rangle_A|0\rangle_B\right) \\ |\Phi^-\rangle &= \frac{1}{\sqrt{2}}\left(|0\rangle_A|0\rangle_B - |1\rangle_A|1\rangle_B\right) \qquad |\psi^-\rangle = \frac{1}{\sqrt{2}}\left(|0\rangle_A|1\rangle_B - |1\rangle_A|0\rangle_B\right) \ . \end{aligned} \tag{2.11}$$

This can be generalized to high dimensional entanglement for systems with $N > 2$ orthogonal states. The N-dimensional Bell basis can be written as:

$$|\Psi\rangle_{AB}^{mn} = \frac{1}{\sqrt{N}} \sum_{k=0}^{N-1} e^{\frac{2\pi i}{d} nk} |k\rangle_A |k + m \ (\mathrm{mod}\, N-1)\rangle_B \ . \tag{2.12}$$

Here, $(n,\ m) \in \{0, 1, ...,\ N-1\}^2$. For example, for a quantum system with $N = 4$ energy levels there are 16 Bell basis states:

$$\begin{aligned} |\Psi\rangle_{AB}^{00} &= \frac{1}{2}\left(|0\rangle_A|0\rangle_B + |1\rangle_A|1\rangle_B + |2\rangle_A|2\rangle_B + |3\rangle_A|3\rangle_B\right) \\ |\Psi\rangle_{AB}^{01} &= \frac{1}{2}\left(|0\rangle_A|0\rangle_B + i|1\rangle_A|1\rangle_B - |2\rangle_A|2\rangle_B - i|3\rangle_A|3\rangle_B\right) \\ &\vdots \\ |\Psi\rangle_{AB}^{33} &= \frac{1}{2}\left(|0\rangle_A|3\rangle_B - i|1\rangle_A|0\rangle_B - |2\rangle_A|1\rangle_B + i|3\rangle_A|0\rangle_B\right) \ . \end{aligned} \tag{2.13}$$

2.2.1. Quantifying Entanglement

There are various metrics to quantify entanglement in a quantum system. The metrics we encounter in this thesis are:

1. **Fidelity.** This metric measures how similar two quantum states are. Thus, it allows us to compare any state to a Bell basis state to see how similar this state is to the Bell basis state. Given two density matrices ρ and σ, the fidelity is defined as:

$$F(\rho, \sigma) = \left(\mathrm{Tr}\left(\sqrt{\sqrt{\rho}\sigma\sqrt{\rho}}\right)\right)^2 \ . \tag{2.14}$$

   In the case of two pure states $|\psi\rangle$ and $|\phi\rangle$ the fidelity simplifies to:

$$F(\psi, \phi) = |\langle\psi|\phi\rangle|^2 \ . \tag{2.15}$$

   From the last expression, we see that the fidelity indeed measures the similarity. If the pure states are completely orthogonal, the inner product returns zero. If the states are the exactly the same the fidelity is $F = 1$ and in general the closer $|\psi\rangle$ is to $|\phi\rangle$, the closer the fidelity is to 1. For $F > \frac{1}{2}$ the quantum state is considered entangled.
2. **Schmidt rank.** According to the Schmidt decomposition, every bipartite quantum state can be written in the form:

$$|\psi\rangle_{AB} = \sum_{i=1}^{\min(d_A, d_B)} \lambda_i |u_i\rangle_A \otimes |v_i\rangle_B \ . \tag{2.16}$$

For some bases $\{|u_i\rangle_A\}$ and $\{|v_i\rangle_B\}$, $|u_i\rangle$ and $|v_i\rangle$ are the Schmidt vectors and λ_i are the Schmidt coefficients. d_A and d_B denote the dimensions of systems A and B. The Schmidt rank S is defined as the number of non-zero Schmidt coefficients and it can be used to see whether a state is separable or not: iff $S = 1$, the state is separable and thus not entangled [11]. This metric is less specific than fidelity since it only takes into account the number of non-zero Schmidt coefficients and not the specific values of these coefficients. Even if the Schmidt rank is maximized the fidelity may not equal one.

2.2.2. Applications of Entanglement

The advantage of entanglement in quantum algorithms is not immediately obvious. By itself, entanglement does not allow for the transmission of information. This is called the no-communication theory [38] and to see this we consider the following situation. Alice and Bob are far apart again and Alice wants to send Bob a message. Their qubits are entangled, the joint state is $|\Phi^+\rangle = \frac{1}{\sqrt{2}}(|00\rangle_{AB} + |11\rangle_{AB})$. If Alice measures her qubit in the computational basis, both qubits collapse to either $|0\rangle$ or $|1\rangle$. However, only Alice knows the outcome of the measurement. If she wants to communicate with Bob, she still has to communicate the result classically. Thus, entanglement cannot be used to communicate faster than we do already.

Entanglement does allow two systems two to be correlated stronger than classically possible as has been demonstrated in various experiments with Bell tests [1][24]. This property can be used as a resource in quantum algorithms, for example to distribute secret keys to communicate in an information theoretically secure way with quantum key distribution [18]. Entanglement can also be used to execute algorithms faster [28] and for quantum sensing [23].

2.3. Linear Optics Quantum Computing (LOQC)

In 2000 Knill, Laflamme and Milburn (KLM) [29] showed that universal quantum computation with photons being the carrier of quantum information is possible by using linear optical elements and additional ancillary photons. There are many platforms being researched nowadays that can also do universal quantum computation. The advantage of photons is that they are very suitable for quantum communication: photonic qubits are used to communicate between remote quantum nodes. They are able to carry quantum information over long distances and they are robust to bit-flip errors when they are encoded in time-bins [10]. In this section, we discuss linear optical elements and how they manipulate the states of photons. This discussion is largely based on chapters from Gerry and Knight [21].

Linear Optical Elements

A beam splitter is a partially reflecting mirror that splits the incoming light into two outgoing beams: reflected light and transmitted light. In the quantum regime we consider a photon source that produces one or a few photons. In this regime, the beam splitter is described by Fock states that represent the input and output ports: $|n\rangle_i$ with n the number of photons at a port i, where $i = 0,1,2,3$. Fock states are manipulated via creation and annihilation operators: $\hat{a}_i^\dagger$ and $\hat{a}_i$ respectively. The actions of these operators on the Fock states are:

$$\begin{aligned} \hat{a}_i^\dagger |n\rangle &= \sqrt{n+1}\,|n+1\rangle \\ \hat{a}_i |n\rangle &= \sqrt{n}\,|n-1\rangle \quad . \end{aligned} \tag{2.17}$$

The creation operator adds a photon to the Fock state and the annihilation operator removes a photon. The relation between the input ports and output ports of a beam splitter can be described in terms of creation and annihilation operators: input modes $\hat{a}_0$ and $\hat{a}_1$ transform into output modes $\hat{a}_2$ and $\hat{a}_3$ as follows:

$$\begin{aligned} \hat{a}_2 &= r\hat{a}_1 + t\hat{a}_0 \\ \hat{a}_3 &= t\hat{a}_1 + r\hat{a}_0 \ . \end{aligned} \tag{2.18}$$

Or equivalently in matrix form:

$$\begin{bmatrix} \hat{a}_2 \\ \hat{a}_3 \end{bmatrix} = \begin{bmatrix} t & r \\ r & t \end{bmatrix} \begin{bmatrix} \hat{a}_0 \\ \hat{a}_1 \end{bmatrix} = \tau \begin{bmatrix} \hat{a}_0 \\ \hat{a}_1 \end{bmatrix} \quad . \tag{2.19}$$

Here, r and t are the reflectances and transmittances and τ is the transfer matrix. We give a depiction of the beam splitter and annihilation operators in Figure 2.2.

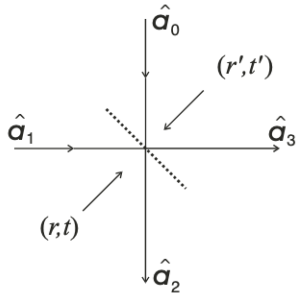

Figure 2.2: Quantum mechanical depiction of the beam splitter.

Since photons are bosons, they should satisfy the bosonic commutation relations:

$$[\hat{a}_i, \hat{a}_j^\dagger] = \delta_{ij}, \quad [\hat{a}_i, \hat{a}_j] = [\hat{a}_i^\dagger, \hat{a}_j^\dagger] = 0 \qquad \wedge \quad (i,j) \in \{0,1,2,3\}^2 \ . \tag{2.20}$$

Substituting the transformation of the beam splitter Eq. (2.18) into the commutation relations Eq. (2.20) yields constraints for the beam splitter matrix in Eq. (2.19). In its most general form we can write the beam splitter matrix as:

$$\tau = e^{i\phi_0} \begin{bmatrix} \cos\theta e^{i\phi_T} & \sin\theta e^{i\phi_R} \\ -\sin\theta e^{-i\phi_R} & \cos\theta e^{-i\phi_T} \end{bmatrix} \quad . \tag{2.21}$$

Here, $2 \cdot \phi_T$ is the phase difference between the transmitted beams and $2 \cdot \phi_R$ is the phase difference between the reflected beams. ϕ_0 is a global phase that we assume to be $\phi_0 = 0$ from now on. θ is related to the transmittance and reflectance as $t = \cos\theta$ and $r = \sin\theta$.

Symmetric Beam Splitters

By choosing the parameters ϕ_T and ϕ_R, we can construct several types of beam splitters. We choose $\phi_T = 0$ and $\phi_R = -\frac{\pi}{2}$ to find the transfer matrix of a symmetric beam splitter:

$$\begin{bmatrix} \hat{a}_2 \\ \hat{a}_3 \end{bmatrix} = \frac{1}{\sqrt{2}} \begin{bmatrix} \cos\theta & -i\sin\theta \\ -i\sin\theta & \cos\theta \end{bmatrix} \begin{bmatrix} \hat{a}_0 \\ \hat{a}_1 \end{bmatrix} = \cos\theta \hat{I} - i\sin\theta \hat{X} \ . \tag{2.22}$$

This is a rotation around the $\hat{x}$ - axis through an angle of 2θ radians.

50:50 Beam Splitter

In this thesis we use the $50:50$ beam splitter most of the time. Here ϕ_T and ϕ_R differ by a factor $e^{\pm\frac{i\pi}{2}} = \pm i$ and $\theta = \frac{\pi}{4}$. By choosing $\phi_R = \frac{\pi}{2}$, we find the following transfer matrix:

$$\begin{bmatrix} \hat{a}_2 \\ \hat{a}_3 \end{bmatrix} = \frac{1}{\sqrt{2}} \begin{bmatrix} 1 & i \\ i & 1 \end{bmatrix} \begin{bmatrix} \hat{a}_0 \\ \hat{a}_1 \end{bmatrix} \quad . \tag{2.23}$$

Polarizing Beam Splitter

In Section 2.1.1 we discussed various photonic degrees of freedom in which a quantum state can be encoded. Photons encoded in the polarization degree of freedom can be manipulated with polarizing beam splitters polarization (PBs). These beam splitters refract the two polarizations at different angles θ from Eq. (2.22). The difference with normal beam splitters is that light leaving the PBs in one output port has an orthogonal polarization with regard to the other output port.

Phase Shifter

Phase shifters are often used to apply a phase shift to a photon. In the Bloch sphere representation, it applies a rotation of $-\phi$ around the $\hat{z}$-axis. The transfer matrix looks like:

$$U_P(\phi) = \begin{bmatrix} e^{i\phi} & 0 \\ 0 & 1 \end{bmatrix} \quad . \tag{2.24}$$

With a beam splitter and phase shifter combination, the Hadamard gate can be created:

$$H = \begin{bmatrix} 1 & 1 \\ 1 & -1 \end{bmatrix} \quad . \tag{2.25}$$

Creating Single Photons

There are many ways to generate single photons. One way could be to attenuate a laser pulse, for example turning a laser on for a very short time. The resulting state is called a coherent state:

$$|\alpha\rangle = e^{-|\alpha|^2/2} \sum_{n=0}^{\infty} \frac{\alpha^n}{\sqrt{n}} |n\rangle \quad . \tag{2.26}$$

Here $|n\rangle$ represents a Fock state (or number state) where n is the number of photons being emitted. We see that an attenuated laser pulse does not yield a single photon, but rather a superposition of all number states. The mean photon number is $|\alpha|^2$, thus by choosing α we can lower the probability of modes with $n > 1$.

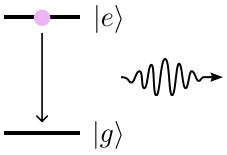

Figure 2.3: Single photon emission.

Alternatively, emitters can generate single photons via spontaneous emission. We give an overview of the two-level optical system in Figure 2.3. There are two energy levels: a ground state and an excited state. A short laser pulse excites the electron occupying the ground state to the excited state. The electron decays radiatively to the ground state and a photon will be emitted.

Delay Lines

Delay lines are used to delay a photon traveling in a spatial mode with n time-bins. For example time bin $|i\rangle$ gets delayed to $|i+n\rangle$.

2.3.1. Universal Quantum Computation with Linear Optics

To achieve universal quantum computation with linear optical elements, we should be able to apply arbitrary single-qubit operations and two-qubit operations. In Chapter 4 Nielsen and Chuang [36] state that any single qubit operation U may be written as:

$$U = e^{i\alpha} R_{\hat{n}}(\beta) R_{\hat{m}}(\gamma) R_{\hat{n}}(\delta) \ . \tag{2.27}$$

Here, $\hat{n}$ and $\hat{m}$ are non-parallel axes, α, β, γ and δ are the appropriate angles and $R_{\hat{n}}(\beta)$ is a gate that applies a rotation of β radians around axis $\hat{n}$. This theorem tells us that if rotations around two non-parallel axes are possible, any single qubit operation can be executed. Thus, phase shifters and symmetric beam splitters are sufficient to achieve arbitrary single-qubit rotations on the Bloch sphere. In Figure 2.4 we give a set-up to create any superposition $|\psi\rangle = \alpha|0\rangle + \beta e^{i\phi}|1\rangle$ by using a photon in an early time-bin $|0\rangle$ and a late time-bin $|1\rangle$. The photon first enters a symmetric beam splitter. With probability $||\alpha|^2$ the photon continues in a straight line and with probability $|\beta|^2$ the photon is reflected into another spatial mode. The reflected photon travels longer through the delay line and a phase shift of ϕ radians is applied. Finally, the two paths are combined the photon encodes a quantum state.

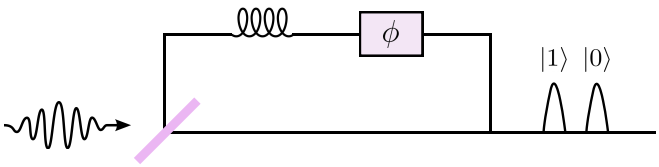

Figure 2.4: Scheme to encode a photon in an arbitrary superposition of two time-bins.

Controlled operations are less straightforward with linear optical elements. Knill, Laflamme and Milburn [29] were the first to propose a probabilistic scheme to implement a two-qubit gate with linear optical elements. They require two ancillary modes and a photon detector to measure the ancillary photon at the end of the scheme. We will not use their set-up for a controlled phase operation in this thesis, but it is an important finding that controlled operations can be implemented with ancillary photons, linear optical elements and photon detectors.

2.4. Quantum Teleportation

In 1993 Bennet et al. [7] proposed a protocol called quantum teleportation that uses entangled qubits as a resource. This protocol allows the transfer of quantum information from one party to another without actually sending the qubit. Suppose Alice wants to transfer the state of her photonic qubit $|\phi\rangle_A$ to Bob, who is a distance L away. Alice could just send her photon to Bob over a quantum communication channel, but that is not very efficient: we know from Section 2.1.2 that the transmission loss increases exponentially with distance. This is the main advantage of quantum teleportation: the particles between which quantum information is transferred do not have to move at all.

Quantum teleportation does require an entangled state as a resource, shared by Alice and Bob. We give the scheme for quantum teleportation in the figure below.

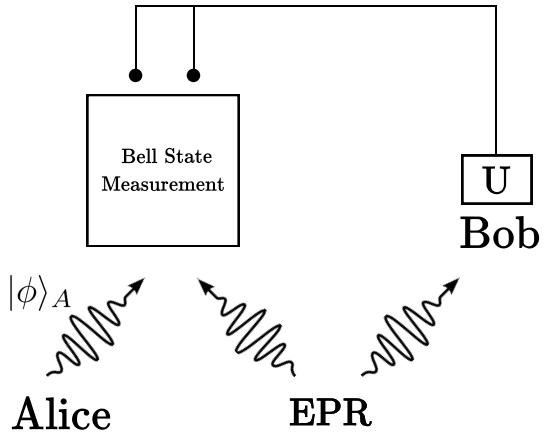

Figure 2.5: Quantum teleportation of the quantum state of a qubit $|\phi\rangle_A$. Alice performs a Bell state measurement on this qubit and the qubit that is entangled with Bob. If the measurement succeeds, Bob applies an outcome-dependent unitary on his photon. Now Bob's qubit encodes the state $|\phi\rangle_A$.

Here, Alice holds a photon in the state $|\phi\rangle_A$. The state can be encoded in many degrees of freedom of the photon but in general it looks like:

$$|\phi\rangle_A = \alpha|0\rangle + \beta|1\rangle \quad . \tag{2.28}$$

Alice and Bob both have one photon of an entangled photon pair. Alice performs a Bell state measurement on her two photons. This projects the particle with her quantum state and the entangled photon into a joint state. She classically communicates the outcome to Bob and with probability $\frac{1}{2}$ Bob can reconstruct $|\phi\rangle_A$ by applying an outcome-dependent local unitary operation. In Section 3.1 we discuss how the Bell state measurement can be implemented if the photons are encoded in two time-bins.

2.5. Optical Switches

The optical switch is the only non-linear element that we encounter in this thesis. It allows us to switch a photon between spatial modes in between time-bins [30]. A photon in an early time-bin will go to one spatial mode and by turning on the optical switch, a photon in the late time-bin switches goes to another spatial mode. We give an overview of the set-up for an optical switch in Figure 2.6.

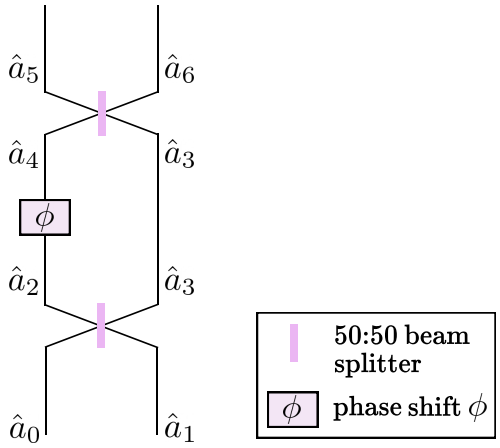

Figure 2.6: An optical switch. A photon enters input mode 0 and input mode 1 is always vacuum. By switching the phase shift between $\phi = 0$ and $\phi = \pi$, the output port of the photon can be chosen.

To see how this works, we consider the transformation of input modes $\hat{a}_0$ and $\hat{a}_1$ into output modes $\hat{a}_5$ and $\hat{a}_6$. Here, we assume that the particle enters input port $\hat{a}_0$ and that input port $\hat{a}_1$ is always a vacuum. After the first $50:50$ beam splitter, the transformation according to Eq. (2.23) is:

$$\begin{aligned} \hat{a}_2 &\to \frac{1}{\sqrt{2}}(\hat{a}_0 + i\hat{a}_1) \\ \hat{a}_3 &\to \frac{1}{\sqrt{2}}(i\hat{a}_0 + \hat{a}_1) \ . \end{aligned} \tag{2.29}$$

Next we apply the phase shifter according to Eq. (2.24):

$$\begin{aligned} \hat{a}_4 &\to \frac{1}{\sqrt{2}}(e^{i\phi}\hat{a}_0 + ie^{i\phi}\hat{a}_1) \\ \hat{a}_3 &\to \frac{1}{\sqrt{2}}(i\hat{a}_0 + \hat{a}_1) \ . \end{aligned} \tag{2.30}$$

After the final beam splitter we find:

$$\begin{aligned} \hat{a}_5 &\to \frac{1}{2}(e^{i\phi}\hat{a}_0 + e^{i\phi}\hat{a}_1 - \hat{a}_0 + i\hat{a}_1) \\ \hat{a}_6 &\to \frac{1}{2}(ie^{i\phi}\hat{a}_0 - e^{i\phi}\hat{a}_1 + i\hat{a}_0 + \hat{a}_1) \ . \end{aligned} \tag{2.31}$$

We control the angle ϕ. If we choose $\phi = 0$, we find:

$$\begin{aligned} \hat{a}_5 &\to \frac{1+i}{2}\hat{a}_1 \\ \hat{a}_6 &\to \frac{2i}{2}\hat{a}_0 = i\hat{a}_0 \ . \end{aligned} \tag{2.32}$$

Since 1 is always a vacuum, the photon will always leave output port 5 for this choice of ϕ. Now we choose $\phi = \pi$. We substitute this in Eq. (2.31) and find:

$$\begin{aligned} \hat{a}_5 &\to \frac{-2}{2}\hat{a}_0 = -\hat{a}_0 \\ \hat{a}_6 &\to \frac{2}{2}\hat{a}_1 = \hat{a}_1 \ . \end{aligned} \tag{2.33}$$

The photon always leaves output port 6. By switching the phase in between time-bins, the spatial mode in which the photon leaves is changed.

3

Literature Review

In this chapter, we start by discussing single-photon and two-photon entanglement protocols as proposed by Barrett and Kok [4]. In higher dimensions, we need an N-dimensional Bell state measurement in order to perform entanglement generation. First of all we aim to give a background on the theoretical limitations of the N-dimensional Bell state measurement. The N-dimensional Bell state measurement can be applied in more protocols, for example many works have considered high-dimensional quantum teleportation as proposed by Bennett et al. [7]. Their implementations of N-dimensional Bell state measurements can be used for N-dimensional entanglement generation. For $N = 2^d$, we herald d entangled qubits at the same time and thus increase the average fidelity for large distances. We summarize previous works towards high-dimensional quantum teleportation.

3.1. Single Photon Entanglement Protocol

One way of generating an entangled qubit pair is with the single-photon entanglement protocol with quantum emitters as described by Barrett and Kok [4]. In this section, we take a closer look at this protocol and how the success probability scales with distance. This discussion is based on the paper by Hermans et al. [25]

Alice and Bob each have a qubit that they want to entangle. We give a visualization of the level structure of their qubits in Figure 3.1. There are two ground state levels, $|0\rangle$ and $|1\rangle$. We see that the transition between the ground state levels can be driven. $|e\rangle$ is the excited level and only the ground state level $|0\rangle$ can be excited to this state. The excited state decays radiatively, therefore $|0\rangle$ is also called the bright state.

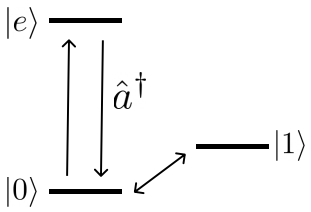

Figure 3.1: Level structure of the qubit on Alice's and Bob's side. The transition between the ground states $|0\rangle$ and $|1\rangle$ can be driven and only $|0\rangle$ can be excited to $|e\rangle$. After this excitation, $|e\rangle$ decays under emission of a photon to $|0\rangle$.

An example of a quantum emitter is the nitrogen-vacancy center which consists of a nitrogen atom next to a vacancy. An electron is trapped in the vacancy and by applying a laser the electron can

be excited depending on its spin state [15]. We give an overview of the single-photon entanglement scheme in Figure 3.2. The BSM is performed with a beam splitter and the creation and annihilation operators $\hat{a}_i$ and $\hat{a}_i^\dagger$ have a subscript i that corresponds to the ports of the beam splitter $i \in \{0,1,2,3\}$. The photon detectors are numbered by 0 and 1. Alice and Bob try to entangle their qubits by each executing the following protocol:

1. Prepare the qubit in the superposition state:

$$\sqrt{\alpha}\,|0\rangle + \sqrt{1-\alpha}\,|1\rangle \quad . \tag{3.1}$$

2. Excite the qubit with an optical pulse. A photon is emitted in time-bin 0 if the electron was in the bright state and it remains dark for $|1\rangle$:

$$\sqrt{\alpha}\,|0\rangle\,|0\rangle_{ph} + \sqrt{1-\alpha}\,|1\rangle\,|\mathrm{vac}\rangle_{ph} \quad . \tag{3.2}$$

3. Send their photon to a middle station where the photons interfere on a beam splitter and are measured with photon detectors at output ports 2 and 3.
4. The middle station communicates to Alice and Bob which detectors have clicked via a classical communication channel. If exactly one of the detectors clicks, the protocol succeeds.

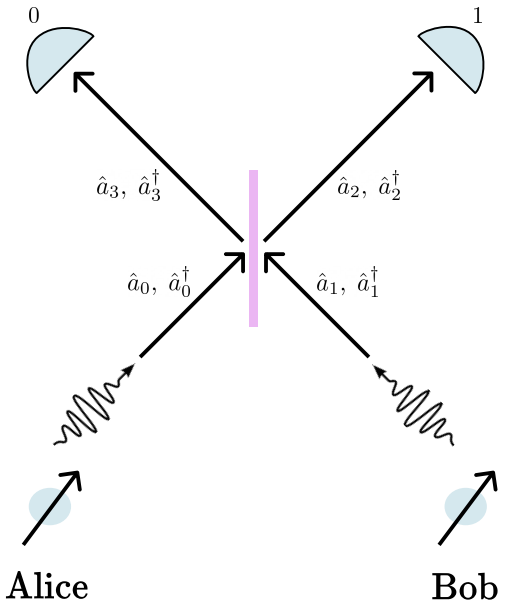

Figure 3.2: In the single-photon entanglement protocol Alice and Bob both emit either no photon or one photon that is entangled with the state of their qubit. A middle station performs a BSM on its incoming photons with a beam splitter and two photon detectors 0 and 1.

The joint state of Alice's and Bob's qubits (indicated by A and B) and their photons (indicated by a and b) before the beam splitter is:

$$\begin{aligned} |\psi\rangle_{ABab} &= \left(\sqrt{\alpha}\,|0\rangle_A\,|0\rangle_a + \sqrt{1-\alpha}\,|1\rangle_A\,|\mathrm{vac}\rangle_a\right) \otimes \left(\sqrt{\alpha}\,|0\rangle_B\,|0\rangle_b + \sqrt{1-\alpha}\,|1\rangle_B\,|\mathrm{vac}\rangle_b\right) \\ &= \alpha\,|00\rangle_{AB}\,|0\rangle_a\,|0\rangle_b + \sqrt{\alpha(1-\alpha)}\left(|10\rangle_{AB}\,|\mathrm{vac}\rangle_a\,|0\rangle_b + |01\rangle_{AB}\,|0\rangle_a\,|\mathrm{vac}\rangle_b\right) \\ &\quad + (1-\alpha)\,|11\rangle_{AB}\,|\mathrm{vac}\rangle_a\,|\mathrm{vac}\rangle_b \quad . \end{aligned} \tag{3.3}$$

We rewrite the input-output relations of photons interfering with the 50 : 50 beam splitter from Eq. (2.23):

$$\begin{bmatrix} \hat{a}_0 \\ \hat{a}_1 \end{bmatrix} = \frac{1}{\sqrt{2}} \begin{bmatrix} 1 & i \\ i & 1 \end{bmatrix} \begin{bmatrix} \hat{a}_2 \\ \hat{a}_3 \end{bmatrix} \quad . \tag{3.4}$$

If photons arrive at input port 0 and 1, photons exit port 2 and 3 in the following way:

$$\begin{aligned} \hat{a}_0^\dagger &\to \frac{1}{\sqrt{2}} \left(\hat{a}_2^\dagger - i\hat{a}_3^\dagger \right) \\ \hat{a}_1^\dagger &\to \frac{1}{\sqrt{2}} \left(-i\hat{a}_2^\dagger + \hat{a}_3^\dagger \right) \quad . \end{aligned} \tag{3.5}$$

After the beam splitter, the photon detectors measure either zero, one or two photons. This measurement projects the state of the matter qubits in a state that depends on how many photons are measured and at which detector. For each scenario, we define the projection of the photons in terms of the photon detector that clicked: d_0 and d_1 both can be 0 or 1 depending on the detector at which the photon is measured.

One Click
If one of the detectors clicks, a photon is measured at some detector d_0: $|0\rangle$ and no photon at the other detector d_1: $|\mathrm{vac}\rangle$. This projects the joint state in the basis before the beam splitter as follows:

$$\langle P| = \langle 0|_{d_0} \langle \mathrm{vac}|_{d_1} \mathrm{BS} \quad . \tag{3.6}$$

Here, 'BS' corresponds to the effect of the beam splitter. There are two options: either detector 0 clicks ($d_0 = 0$), or detector 1 clicks ($d_0 = 1$).

1. For $d_0 = 0$, the photons project into:

$$\langle P| = \langle 0|_0 \langle \mathrm{vac}|_1 \mathrm{BS} = \frac{1}{\sqrt{2}} \left(\langle 0|_a \langle \mathrm{vac}|_b - i \langle \mathrm{vac}|_a \langle 0|_b \right) \quad . \tag{3.7}$$

Next, we apply the projection to the initial state $|\psi\rangle_{in}$ from Eq. (3.3) to find the output state of the matter qubits:

$$\begin{aligned} \langle P|\psi\rangle_{ABab} = \frac{1}{\sqrt{2}} \left(\langle 0|_a \langle \mathrm{vac}|_b - i \langle \mathrm{vac}|_a \langle 0|_b \right) \Big(& \alpha |00\rangle_{AB} |0\rangle_a |0\rangle_b + \sqrt{\alpha(1-\alpha)} \left(|10\rangle_{AB} |\mathrm{vac}\rangle_a |0\rangle_b + |01\rangle_{AB} |0\rangle_a |\mathrm{vac}\rangle_b \right) \\ & + (1-\alpha) |11\rangle_{AB} |\mathrm{vac}\rangle_a |\mathrm{vac}\rangle_b \Big) = \sqrt{\alpha(1-\alpha)} \cdot \frac{1}{\sqrt{2}} \left(|01\rangle_{AB} - i|10\rangle_{AB} \right) \quad . \end{aligned} \tag{3.8}$$

Alice or Bob applies a local unitary to their qubits to go to the state $|\Psi^+\rangle = \frac{1}{\sqrt{2}} \left(|01\rangle + |10\rangle \right)_{AB}$. The probability to see this detection pattern is the square of the constant in front of the state from Eq. (3.8):

$$p_{1\text{ click}} = |\sqrt{\alpha(1-\alpha)}\,|^2 = \alpha(1-\alpha) \quad . \tag{3.9}$$

Which is maximized for $\alpha = \frac{1}{2}$: $p_{1\text{ click}} = \frac{1}{4}$.

2. For $d_0 = 1$, the photons are projected in a slightly different way but by applying a local unitary on Alice or Bob's side we herald the same Bell state. We project the photons into:

$$\langle P| = \langle 0|_1 \langle \mathrm{vac}|_0 \mathrm{BS} = \frac{1}{\sqrt{2}} \left(-i \langle 0|_a \langle \mathrm{vac}|_b + \langle \mathrm{vac}|_a \langle 0|_b\right) \ . \tag{3.10}$$

The state of Alice and Bob's memory qubits collapses to:

$$\langle P|\psi\rangle_{in} = \sqrt{\alpha(1-\alpha)} \cdot \frac{1}{\sqrt{2}} \left(-i|01\rangle_{AB} + |10\rangle_{AB}\right) \ . \tag{3.11}$$

After Alice or Bob applies a local unitary, they share the Bell state $|\Psi^+\rangle$. The probability for this to happen is the same as Eq. (3.9).

Thus, when exactly one of the detectors clicks the protocol has succeeded and Alice and Bob share the state $|\Psi^+\rangle$ after applying a unitary that is conditional on which detector clicked. The total probability of success is $p_{succ} = 2\alpha(1-\alpha)$ and at most $p_{succ} = \frac{1}{2}$.

Zero Clicks

If no detector clicks, the photons project into:

$$\langle P| = \langle \mathrm{vac}|_0 \langle \mathrm{vac}|_1 \mathrm{BS} = \langle \mathrm{vac}|_a \langle \mathrm{vac}|_b \ . \tag{3.12}$$

The state of Alice and Bob collapses to:

$$\langle P|\psi\rangle_{in} = (1-\alpha)\,|11\rangle_{AB} \ . \tag{3.13}$$

The probability to see this detection pattern is:

$$p_{0\,\mathrm{clicks}} = (1-\alpha)^2 \ . \tag{3.14}$$

The Schmidt rank of the heralded state from Eq. (3.13) is $S_{0\,\mathrm{clicks}} = 1$. Local unitaries applied by Alice and Bob cannot increase $S_{0\,\mathrm{clicks}}$ to the Schmidt rank of a Bell state: $S_{\mathrm{Bell}} = 2$ [36]. Thus, the protocol fails to herald a Bell state if there are no photons detected.

Two Clicks

If the detectors measure two photons, both Alice and Bob emitted a photon. Thus, a photon entered each input port of the 50 : 50 beam splitter. This leads to two-photon interference: the Hong-Ou-Mandel effect [26]. Two photons that arrive at exactly the same time and in general are indistinguishable will exit the beam splitter in the same output port. One detector will click twice (if the detector can measure two photons at the same time). If detector 0 measures both photons, the photons are projected into:

$$\begin{aligned} \langle P| &= \langle 1|_0 \langle 1|_0 \mathrm{BS} = \frac{1}{2} \left(\langle 1|_a - i\langle 1|_b\right) \otimes \left(\langle 1|_a - i\langle 1|_b\right) \\ &= \frac{1}{2} \left(\langle 1|_a \langle 1|_a - 2i\langle 1|_b \langle 1|_a - \langle 1|_b \langle 1|_b\right) \\ &= -2i \langle 1|_a \langle 1|_b \ . \end{aligned} \tag{3.15}$$

In the last line, we only keep the terms that are possible in this scheme: all terms with more than one photon entering the same input port are neglected. We apply this projection to the input state from Eq. (3.3):

$$\langle P|\psi\rangle_{in} = i\alpha\,|00\rangle_{AB} \ . \tag{3.16}$$

Similar to the situation with no clicks, the Schmidt rank of the heralded state is $S_{2\,\text{clicks}} = 1$ instead of $S_{\text{Bell}} = 2$. The protocol fails with probability $p_{2\,\text{clicks}} = \alpha^2$. If the other detector measured both photons, the result is the same up to a global phase factor.

Robustness against loss of one photon

If we could ensure that no photons get lost, the success probability is optimized for $\alpha = \frac{1}{2}$, which gives a total success probability of $p_{succ} = \frac{1}{2}$. However, when photons are transmitted over an optical fiber the probability of successfully transmitting the photon decreases exponentially as a function of distance as described by Eq. (2.9). The single-photon is not very robust to losing a photon since we cannot distinguish between the case where two photons were emitted and one was lost or the case where one photon was emitted and not lost. If one photon is detected but in reality two photons were emitted, the average fidelity of the heralded entangled state with $|\Psi^+\rangle$ is lower than one. To avoid emitting two photons the coefficient α should be small: $\alpha \leq 1$. The success probability decreases as well: $2\alpha(1-\alpha)$. We see that there is a trade-off between the fidelity of the heralded state and the success probability in the single-photon protocol. The two-photon protocol circumvents this trade-off [4], but it requires the successful transmission of two photons.

3.2. Two-Photon Entanglement Protocol

The two-photon protocol is similar to the single-photon protocol [4]. Now, after the first excitation of Alice and Bob's qubits in the second step of the single-photon protocol 3.1, the state of qubits is flipped: $|0\rangle \leftrightarrow |1\rangle$. Next, they both excite their qubit again and there is a probability to emit a photon in a second time-bin.

Alice and Bob send two photons to the middle station. The photons in the first time-bin interfere on a beam splitter. If one of the detectors clicks, we know the protocol has succeeded. However, if two photons were emitted in time-bin 0, the corresponding state is $|00\rangle_{AB}$. With probability γ one of these photons gets lost during transmission. In the second time-bin, the state of Alice and Bob's memory qubits $|00\rangle$ is flipped to $|11\rangle$ and upon excitation it remains dark: none of the detectors click. Thus, even if one photon is measured in the first round, we can distinguish between the case where a single photon is emitted versus two emitted photons followed by the loss of one photon. We do not need to suppress the emission of two photons in this protocol, so the success probability can be maximized: $p_{\text{succ}} = \frac{1}{2}$.

The rate at which entanglement can be generated depends on the loss of photons during transmission. In the single-photon protocol, one photon needs to travel to the middle station in a successful run of the protocol. Thus, the expected number of entanglement attempts scales as $\langle n\rangle_{SP} \sim \frac{1}{\gamma}$. For the two-photon protocol we need two photons to arrive at the middle states so the number of entanglement attempts increases quadratically: $\langle n\rangle_{TP} \sim \frac{1}{\gamma^2}$. To summarize, the fidelity of the heralded state in the two-photon protocol is more robust to photon loss but the number of attempts is quadratically higher than for the single-photon protocol.

3.3. Bell State Measurement in Higher Dimensions

3.3.1. Motivation

In the single-photon and two-photon entanglement protocol, the memory qubits need to stay coherent approximately for the time it takes to create one successful pair: $t_{SP} = \frac{L}{c}$. Here, L is the distance between Alice and Bob. In practice we may want to generate multiple entangled pairs, for example for entanglement purification [6][16]. If the two nodes are far apart, the transmission loss of the photons will be high. In addition to this, there will be other losses that depend on which quantum system is

being used. For example for NV centers many photons are being emitted in the phonon sideband and these photons will have a different frequency than we want. They are unsuited to use for entanglement generation because the photons coming into the middle station need to be indistinguishable. Only 3% of the photons are emitted with the correct frequency in the zero-phonon line [20].

To lower the requirements on the memory time, the single-photon or two-photon entanglement protocol can be executed in parallel as has been demonstrated experimentally [31]. This is called multiplexing and allows the generation of d entangled pairs simultaneously. If we execute the two-photon protocol simultaneously d times, the probability for all protocols to succeed and to generate d pairs at the same time is:

$$p_{\text{all}} = \left(p_t^2 \cdot p_{\text{succ}}\right)^d = \frac{e^{-2dL/L_{att}}}{2^d} \quad . \tag{3.17}$$

Here, p_t is the probability to transmit a photon over a distance L. We consider the two-photon entanglement protocol, hence we use the transmission probability squared since two photons need to survive the transmission. The term p_{succ} is the success probability of the two-photon entanglement protocol. The total probability p_{all} decreases exponentially with distance and the required number of entangled pairs and this negatively impacts the rate at which entangled pairs are generated. In general the probability to generate x pairs with $x \leq d$ in the first execution of the protocols is given by the probability mass function:

$$p_x = \frac{d!}{x!(d-x)!} \left(p_t \cdot p_{\text{succ}}\right)^x \left(1 - p_t \cdot p_{\text{succ}}\right)^{d-x} \quad . \tag{3.18}$$

During the time it takes to generate the remaining pairs $d-x$, the generated pairs dephase. We can circumvent this by heralding that all pairs are generated at the same time in every successful run of the protocol. This can be done by performing a Bell state measurement in higher dimensions.

The Bell state measurement is used in many applications, for example high-dimensional quantum teleportation. In our case, we want to use the Bell state measurement for N-dimensional entanglement generation between remote nodes in higher dimensions. This would allow us to generate d entangled pairs at the same time for $N = 2^d$ which means that the qubits in the register only have to stay coherent during the time it takes to execute the protocol once: $t = \frac{L}{c}$. We start by discussing the theoretical limitations of the Bell state measurement and then we discuss recent work towards high-dimensional quantum teleportation.

3.3.2. Limitations

The entanglement protocols from the previous sections do not perform a complete Bell state measurement since the measurement at the middle station cannot distinguish all Bell states as given by Eq. (2.11). They do not measure in the basis of the following Bell states, with modes that would contain two photons in the same time-bin:

$$\begin{aligned} |\Phi^+\rangle &= \frac{1}{\sqrt{2}} \left(|0\rangle_A |0\rangle_B + |1\rangle_A |1\rangle_B\right) \\ |\Phi^-\rangle &= \frac{1}{\sqrt{2}} \left(|0\rangle_A |0\rangle_B - |1\rangle_A |1\rangle_B\right) \quad . \end{aligned} \tag{3.19}$$

The beam splitter removes the which-path information of the incoming photons. When only one photon is emitted, we do not know from which side it came and thus the entangled state is heralded. For $|\Phi^+\rangle$ and $|\Phi^-\rangle$, the term $|0\rangle_A |0\rangle_B$ corresponds to two emitted photons and $|1\rangle_A |1\rangle_B$ corresponds to zero emitted photons. Removing the which-path information does not work since the measurement collapses the

state to the mode with two photons or no photons.

Previous works have proved important limitations of performing Bell state measurements in higher dimensions. Calsamiglia [12] showed in 2002 that it is impossible to perform a BSM for dimensions higher than 2 with just 2 photons. More generally, he presents a proof that the Schmidt rank of the heralded state can at most equal the number of initial particles. The Schmidt rank of an N-dimensional entangled state is N and therefore the Bell state measurement needs N input photons. For entanglement generation we always have one photon coming from Alice's side and one photon from Bob's side. Thus, the minimum number of ancillary photons required is $N-2$.

Research has been done to the possibility of deterministic discrimination of Bell states: Calsamiglia and Lütkenhaus prove that the success probability of entangling two qubits without ancillary photons is upper bounded by $\frac{1}{2}$ [13]. Lütkenhaus et al. [33] show that it is impossible to perform a deterministic BSM with linear elements, even with many ancillary photons. However in theory the success probability does converge to 1 when infinitely many ancillary photons are used, as Dusek [17] showed. By combining the ancillary photons into entangled states, the success probability scales with the number of initial particles x as: $p_{\text{succ}} = \left(\frac{x}{x+1}\right)^2$. While it is very interesting, it is not practical to implement: the complicated set-up and a large number of required ancillary photons in complex entangled states would lead to many required resources and errors in practice.

Main Challenges

To summarize, the main challenges for performing a Bell state measurement in higher dimensions are:

1. It is impossible to perform a deterministic BSM with linear optical elements and ancillary photons.
2. The partial BSM can only be implemented with ancillary photons as resources. In order to perform an N-dimensional partial BSM, N initial particles are required.

Note that in the rest of this thesis we follow the convention from related literature and we use 'Bell state measurement' or 'BSM' instead of 'partial Bell state measurement'.

3.3.3. Existing Schemes

By using non-linear elements, Bell state measurements can in theory be performed deterministically in higher dimensions. The protocol proposed by Yunzhe et al. [50] generates d entangled pairs at the same time, thereby reducing the scaling of the coherence time to $t \sim \frac{L}{c}$ again. However the implementation outlined in the paper of Yunzhe et al. requires d emitters strongly coupled to optical resonators to enable spin-photon gate operations.

In two dimensions, previous works demonstrate complete Bell state measurements to generate one qubit pair [34]. Kim et al. [27] use non-linear crystals for the Bell state measurement but the efficiency of the measurement remains low: of the order of 10^{-10}.

This motivates research into performing a Bell state measurement with linear optical elements. Linear optical elements are widely used and while photons can be lost as well, the errors are usually smaller than for non-linear optical elements. Previous works have proposed schemes for a Bell state measurement in higher dimensions in the context of quantum teleportation.

Quantum Teleportation in High Dimensions

There have been many experimental demonstrations of quantum teleportation with a photonic qubit, for example the teleportation of a polarization encoded photon [9][49], atoms [2], nitrogen-vacancy centers [39], trapped ions [42] and superconducting circuits [45]. In high dimensions, we want to teleport an N-dimensional state $|\phi\rangle_A = \sum_{k=0}^{N-1} \alpha_k |k\rangle$ from Alice to Bob, without sending the photon that encodes this state directly to Bob. We give an overview of high-dimensional quantum teleportation in Figure 3.3.

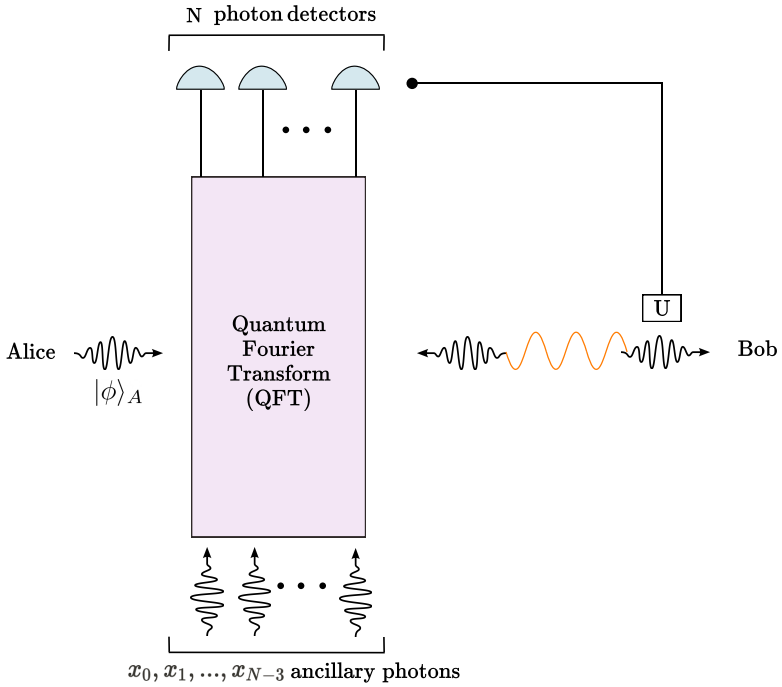

Figure 3.3: Quantum teleportation of an N-dimensional state $|\phi\rangle_A$. Alice performs a QFT on the qudit that is to be teleported, $N-2$ ancillary photonic qudits in a state depending on the protocol and a photonic qudit that is entangled with Bob's photonic qudit. After the QFT the photons are measured. If they are all detected in different time-bins, a unitary operation U conditional on the detectors that clicked is applied on Bob's photonic qudit and Bob's qudit now encodes $|\phi\rangle_A$.

Alice and Bob share a pair of qudits that are entangled in N dimensions and Alice performs a N-dimensional Bell state measurement on her entangled photon, the photon that encodes $|\phi\rangle_A$ and $N-2$ ancillary photons. In previous works, the Bell state measurement is implemented with an N-dimensional quantum Fourier transform followed by N photon detectors. The main difference between these protocols is the input state of the ancillary photons.

Luo et al. [32] have demonstrated experimental 3-dimensional quantum teleportation of a quantum state encoded in the spatial modes of a photon. We give the set-up of their experiment in Figure 3.4. Since there are 3 photons on Alice's side and 1 photon on Bob's side, there are 12 spatial modes in total. To apply the quantum Fourier transform they also use the polarization of the photons and linear optical elements such as wave plates and polarizing beam splitters. The input state of the ancillary photon is an equal superposition state:

$$|\text{anc}\rangle = \frac{1}{\sqrt{3}} (|0\rangle + |1\rangle + |2\rangle) \quad . \tag{3.20}$$

The Bell state measurement succeeds when N photons are measured in different time-bins. In 3 dimen-

sions, their protocol succeeds for all combinations of detectors that can click. Luo et al. show that this leads to a theoretical success probability of $p_{\text{succ}} = \frac{2}{9}$. In general, the success probability scales with dimensions as $p_{\text{tot, up}} = \frac{N!}{N^N}$. Note that this is an upper bound and it has not been proved that the upper bound can be achieved for any dimension. One disadvantage of their protocol is that they require an additional energy level on Bob's side to go to the 3-dimensional state.

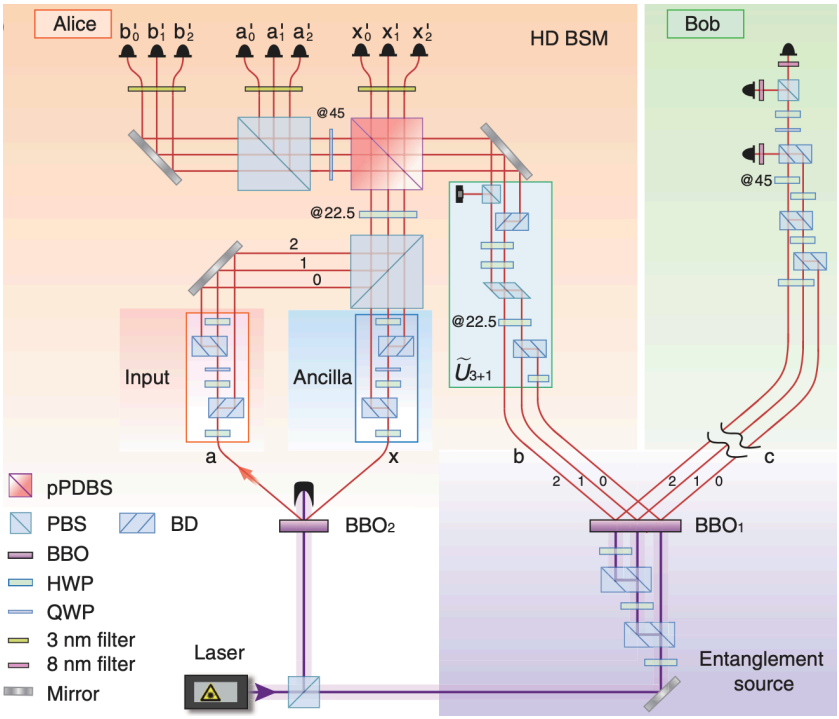

Figure 3.4: Set-up of the protocol of Luo et al. [32] for experimental 3-dimensional quantum teleportation.

Another scheme is proposed by Zhang et al. [48] that we call the permutation protocol in the rest of this thesis. We give an overview of their set-up in arbitrary dimensions in Figure 3.5. They prepare the ancillary photons $a_{1\,i}, a_{2\,i}, ..., a_{N-1\,i}$ in a superposition state of all time-bin permutations, which is an entangled state:

$$|\text{anc}\rangle = \frac{1}{\sqrt{N!}} \sum_{i_0 i_1, ..., i_{N-1} \in P[N]} |i_0 i_1 ... i_{N-1}\rangle_{a_{1\,i}, a_{2\,i}, ..., a_{N-1\,i}} \quad . \tag{3.21}$$

The part lined with red in the figure below describes the Bell state measurement that heralds whether the quantum teleportation was successful. The protocol succeeds when the Bell state measurement selects terms where all photons are in different time-bins. By only inputting modes for the ancillary photons where they are in different time-bins for sure, the success probability p_{U} of the Bell state measurement is boosted. However, in order to create the state of the ancillary photons, their implementation requires $N-2$ extra entangled pairs. One photonic qudit of each pair is measured in the Bell basis with a second N-dimensional Bell state measurement (in the figure indicated with 'V') in order to herald the state from Eq. (3.21). The probability of success of this Bell state measurement is the same as in the protocol of Luo et al.: $p_{\text{V}} = \frac{N!}{N^N}$. Since this success probability needs to be multiplied with p_{U}, the success probability of the total scheme still decreases exponentially with dimension.

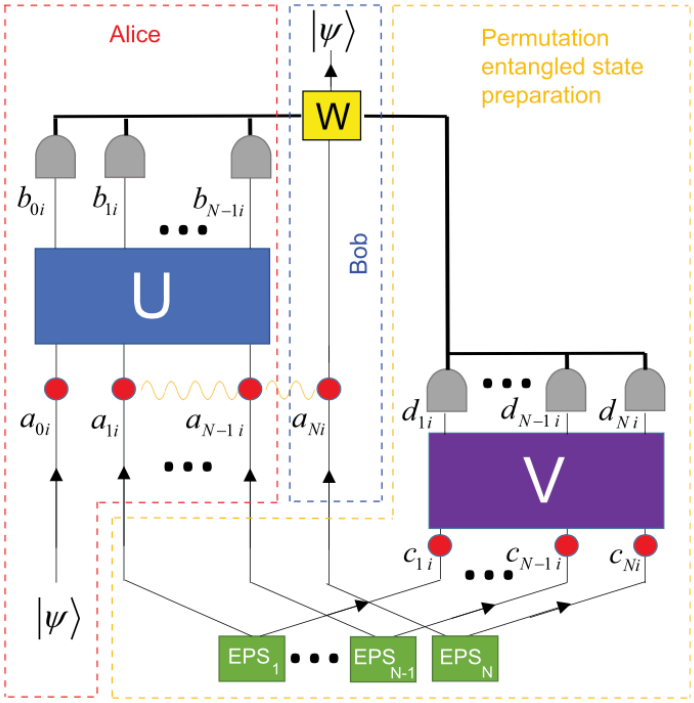

Figure 3.5: Set-up of the theoretical permutation protocol of Zhang et al. [48] to perform quantum teleportation of an N-dimensional quantum state $|\psi\rangle$.

We give a few values for the success probability of state preparation p_{prep}, the teleportation p_{tel} and the total success probability p_{tot} in Table 3.1 as given in [48]:

dimension N	3	4	5	6
p_{prep}	0.22 (2/9)	0.09 (3/32)	0.19 (24/125)	0.02 (5/324)
p_{tel}	0.11 (1/9)	0.15 (5/32)	0.04 (1/25)	0.06 (1/18)
$p_{\text{tot}} = p_{\text{tel}} \cdot p_{\text{prep}}$	0.02 (2/81)	0.01 (15/1024)	0.01 (24/3125)	0.001 (5/5832)

Table 3.1: Success probability of the ancillary state preparation, teleportation and the total success probability of the permutation protocol proposed by Zhang et al. [48].

4

N-Dimensional Entanglement Protocol with All Input Modes

The paper of Luo et al. [32] presents a protocol for high-dimensional entanglement generation with photonic qudits encoded in spatial modes and polarization. In this chapter, we outline a protocol that is an adaptation of the protocol of Luo et al. To keep track of the various protocols that we discuss in this thesis we call the protocol we propose here the all-input modes protocol. We use their implementation of the N-dimensional Bell state measurement to generate high-dimensional entanglement. Note that for $N = 2^d$ the generated entangled state with our protocol can be written as d Bell pairs that are simultaneously generated.

Luo et al. use photons encoded in spatial modes. The number of spatial modes and photon detectors necessary fans out: they both scale as $\mathcal{O}(N^2)$. We propose an implementation with time-bins instead of spatial modes. This gives a quadratic speedup of required hardware elements to $\mathcal{O}(N)$. The Bell state measurement is implemented with a quantum Fourier transform combined followed by a measurement of all photons. Thus, in Section 4.4 we describe research that has been conducted towards using linear optical elements for implementing the quantum Fourier transform, which maps the input states to the Bell basis. Luo et al. teleport a 3-dimensional state from a photon to another photon. Since we want to entangle qudit registers, we need to entangle both qudit registers with a photonic qudit. The N-dimensional Bell state measurement subsequently swaps the entanglement of the qudits with photons to the two qudit registers. We propose two methods to create the qudit-photon entanglement that we need in Sections 4.5 and 4.6.

First, we give a description of our protocol and we present the proof for arbitrary dimensions. Also, we discuss the scaling of success probability with dimension N and we give an upper and lower bound.

4.1. Description of the Protocol

Alice and Bob both have a qudit register with N energy levels that they want to entangle in one successful run of the protocol. Here N can be any natural number $N \geq 2$. If $N = 2^d$, the state shared by Alice and Bob in case of success can be written as d Bell pairs in two dimensions. They execute the following steps as illustrated in Figure 4.1:

1. Alice and Bob start with a superposition of their N energy levels:

$$|\psi\rangle = \frac{1}{\sqrt{N}} \sum_{k=0}^{N-1} |k\rangle \quad . \tag{4.1}$$

2. Alice and Bob entangle each mode $|k\rangle$ with the presence of a photon in the k-th time-bin, as we later describe in Section 4.5 and 4.6. For example, the state of Alice is:

$$|\psi\rangle_{Aa} = \frac{1}{\sqrt{N}} \sum_{k=0}^{N-1} |k\rangle_A |k\rangle_a \quad . \tag{4.2}$$

3. The $N-2$ ancillary photons $x_0, x_1, ..., x_{N-3}$ are prepared in an equal superposition state:

$$|\psi\rangle_{x_0 x_1 ... x_{N-3}} = \frac{1}{\sqrt{N^{N-2}}} \bigotimes_{j=0}^{N-3} \sum_{k=0}^{N-1} |k\rangle_{x_j} \quad . \tag{4.3}$$

4. The photons from Alice and Bob and $N-2$ ancillary photons go to a middle station where they undergo a Bell state measurement. The Bell state measurement is implemented with an N-dimensional quantum Fourier transform and N photon detectors.
5. The middle station classically sends the detection pattern to Alice and Bob.
6. Bob applies the unitary operation from Eq. (4.9) to his qudit. Note that this unitary operation requires one additional energy level.
7. Bob reads out the additional energy level: if the state collapses to the additional energy level, the protocol failed. Bob communicates this to Alice in a classical way and they start over. If the state does not collapse to the additional energy level Alice and Bob continue to step 8.
8. If all photons are measured in different time-bins at the same detector, the time-bin information has been removed and the protocol has succeeded. In this case, either Alice or Bob applies the outcome-dependent local unitary operation $U(d_0, d_1, ..., d_{N-1})$. Here d_i represent the number of the detector at which photon i is measured. Otherwise, the protocol is repeated.

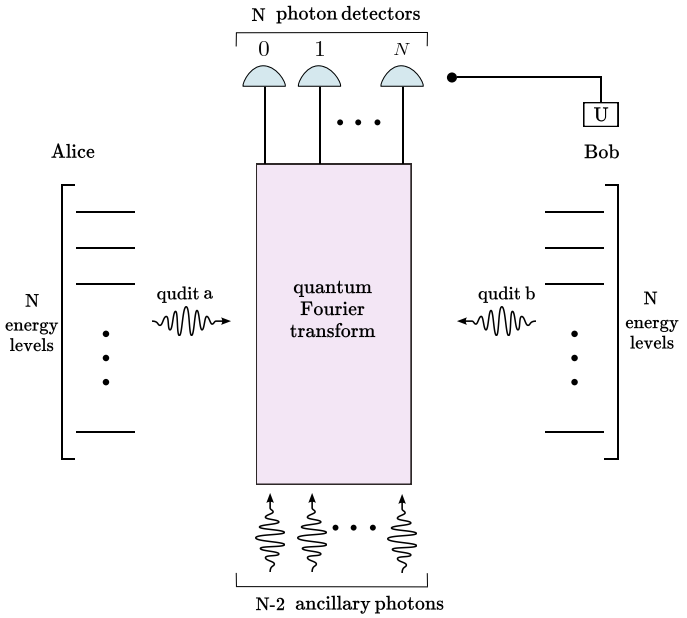

Figure 4.1: High-level overview of the generation of N-dimensional entanglement with the all-input modes protocol. Alice and Bob entangle their qudit register with a photonic qudit encoded in N time-bins. At the middle station the Bell state measurement is performed on the photons from Alice, Bob and $N-2$ ancillary photons. Bob applies a unitary operation U to his register depending on the detection pattern.

4.2. Proof for Arbitrary Dimensions

In this section we show that this protocol indeed creates an N-dimensional entangled state and we give a lower and upper bound on the success probability in arbitrary dimensions.

In step 4 of the all-input modes protocol 4.1 all photons arrive at the middle station. The joint state before the Bell state measurement is:

$$|\psi\rangle_{ABabx_0x_1\ldots x_{N-3}} = \frac{1}{\sqrt{N}}\sum_{k=0}^{N-1}|k\rangle_A|k\rangle_a \otimes \frac{1}{\sqrt{N}}\sum_{l=0}^{N-1}|l\rangle_B|l\rangle_b \otimes \frac{1}{\sqrt{N^{N-2}}}\bigotimes_{j=0}^{N-3}\sum_{m=0}^{N-1}|m\rangle_{x_j} \quad . \tag{4.4}$$

Here, we indicate the state of Alice's qudit with subscript A, the state of Bob's qudit with B and the photonic qudits of Alice's and Bob's side are respectively denoted by a and b.

In step 4, the middle station applies the N-dimensional quantum Fourier transform to photons a, b and x_0 to x_{N-3} in the following way:

$$\begin{aligned}
|i\rangle_0 &\rightarrow \frac{1}{\sqrt{N}}\left(|i\rangle_a + |i\rangle_b + |i\rangle_{x_0} + \ldots + |i\rangle_{x_{N-3}}\right)\\
|i\rangle_1 &\rightarrow \frac{1}{\sqrt{N}}\left(|i\rangle_a + \omega|i\rangle_b + \omega^2|i\rangle_{x_0} + \ldots + \omega^{N-1}|i\rangle_{x_{N-3}}\right)\\
|i\rangle_2 &\rightarrow \frac{1}{\sqrt{N}}\left(|i\rangle_a + \omega^2|i\rangle_b + \omega^4|i\rangle_{x_0} + \ldots + \omega^{2(N-1)}|i\rangle_{x_{N-3}}\right)\\
&\vdots\\
|i\rangle_{N-1} &\rightarrow \frac{1}{\sqrt{N}}\left(|i\rangle_a + \omega^{N-1}|i\rangle_b + \omega^{2(N-1)}|i\rangle_{x_0} + \ldots + \omega^{(N-1)(N-1)}|i\rangle_{x_{N-3}}\right) \quad .
\end{aligned} \tag{4.5}$$

Here, $\omega = e^{2\pi i/N}$ and $0,1,\ldots,N$ are the output spatial modes corresponding to the numbers of the detectors as we see in Figure 4.1. Next we only consider the case where all photons are measured in different time-bins but at the same detector d. We write the quantum Fourier transform in terms of a general detector $d \in \{0,1,\ldots,N-1\}$ where all photons are measured.

$$|i\rangle_d \rightarrow \frac{1}{\sqrt{N}}\left(|i\rangle_a + \omega^d|i\rangle_b + \omega^{2d}|i\rangle_{x_0} + \omega^{3d}|x_1\rangle + \ldots + \omega^{d(N-1)}|i\rangle_{x_{N-3}}\right) \quad . \tag{4.6}$$

The photons are all measured in different time-bins i at detector d. To see how the input state is projected, we apply the quantum Fourier transform to this projection. The projection of photons in the basis before the Bell state measurement is:

$$\begin{aligned}
\langle P|_{abx_0x_1\ldots x_{N-3}} &= \bigotimes_{i=0}^{N-1}\langle i|_d \,\mathrm{QFT} = \bigotimes_{i=0}^{N-1}\frac{1}{\sqrt{N}}\left(\langle i|_a + \omega^d\langle i|_b + \omega^{2d}\langle i|_{x_0} + \ldots + \omega^{d(N-1)}\langle i|_{x_{N-3}}\right)\\
&= \frac{\omega^{d+2d+3d+\ldots+d(N-1)}}{\sqrt{N^N}}\sum_{\{i_0,i_1,\ldots,i_{N-1}\}\in P[N]}\langle i_0|_a\langle i_1|_b\langle i_2|_{x_0}\ldots\langle i_{N-1}|_{x_{N-3}} \quad .
\end{aligned} \tag{4.7}$$

Here $P[N]$ is the full permutation group of the set $\{0,1,\ldots,N-1\}$. The full expression of Eq. (4.7) should contain all photon combinations, including modes with multiple photons in the same spatial mode. This is impossible in our protocol since we only have one photon per input spatial mode. Thus, we only keep the terms corresponding to one photon in each spatial mode and this leaves us with a superposition of all possible permutations of time-bins.

Next, we apply the projection of Eq. (4.7) to the input state from Eq. (4.4). We arrive at the state that Alice's and Bob's qudits are projected into in case of success.

$$|\psi\rangle_{out} = \langle P|_{abx_0x_1\ldots x_{N-3}} |\psi\rangle_{ABabx_0x_1\ldots x_{N-3}} = \frac{\omega^{d\cdot N(N-1)/2}}{\sqrt{N^N}\cdot\sqrt{N^N}} \sum_{j_1,j_2\in\{0,1,\ldots,N\}\,\wedge\, j_1\neq j_2} |j_1\rangle_A\,|j_2\rangle_B \quad . \tag{4.8}$$

Alice and Bob's qudits are in the superposition state of all modes $|j_1\rangle_A$ and $|j_2\rangle_B$ for $j_1 \neq j_2$. To go to a maximally entangled state, we have to apply the operation T_N to Bob's qudits. To make this transformation unitary, we need one extra energy level on Bob's side: U_{N+1}.

$$T_N = \begin{bmatrix} 2-N & 1 & \ldots & 1 \\ 1 & 2-N & \ddots & 1 \\ \vdots & \ddots & \ddots & \vdots \\ 1 & 1 & \ldots & 2-N \end{bmatrix} \quad \rightarrow \quad U_{N+1} = \frac{1}{N-1} \begin{bmatrix} 2-N & 1 & \ldots & 1 & \sqrt{N-2} \\ 1 & \ddots & \ddots & \vdots & \vdots \\ \vdots & \ddots & \ddots & 1 & \vdots \\ 1 & \ldots & 1 & 2-N & \sqrt{N-2} \\ \sqrt{N-2} & \ldots & \ldots & \sqrt{N-2} & -1 \end{bmatrix} \quad . \tag{4.9}$$

After applying this unitary operation, Bob measures the additional energy level. The state of Bob's qudits does not collapse to the additional energy level with probability:

$$p = 1 - \left| \frac{\omega^{d\cdot N(N-1)/2}\sqrt{N-2}}{N^N} \right|^2 \tag{4.10}$$

Alice and Bob finally share the N-dimensional entangled state $|\Psi\rangle_{ND}$:

$$|\Psi\rangle_{ND} = I^A \otimes U^B_{N+1}\,|\psi\rangle_{out} = \boxed{\frac{\omega^{d\cdot N(N-1)/2}\sqrt{N}}{N^N}\cdot\frac{1}{\sqrt{N}}\sum_{j=0}^{N-1}|j\rangle_A\,|j\rangle_B} \quad . \tag{4.11}$$

4.3. Success Probability

For the probability of success of one detection pattern with all photons in different time-bins and at the same detector, we square the constant from Eq. (4.11) and multiply by p from Eq. (4.10):

$$\begin{aligned} p_{suc,1} &= \left| \frac{\omega^{d\cdot N(N-1)/2}\sqrt{N}}{N^N} \right|^2 \cdot \left(1 - \left| \frac{\omega^{d\cdot N(N-1)/2}\sqrt{N-2}}{N^N} \right|^2 \right) \\ &= \frac{1}{N^{2N-1}} - \frac{N-2}{N^{4N-1}} \quad . \end{aligned} \tag{4.12}$$

The number of detectors is N, so all photons can be measured in different time-bins at N different detectors. Thus, we multiply the probability of success of one detection pattern $p_{suc,1}$ by N to get the total success probability p_{suc}:

$$p_{suc} = \frac{N}{N^{2N}} - \frac{N(N-2)}{N^{4N}} \quad . \tag{4.13}$$

Note that this is the probability of success if all photons need to be measured at the same detector for the protocol to succeed. Luo et al. [32] have shown that for 3 dimensions the successful Bell state

measurement can be performed for all different time-bin detections independent of the detector. By applying an outcome-dependent controlled unitary to Bob's qudit, the protocol succeeds for all detection patterns as long as all photons are measured in different time-bins. However, they do not prove that this is possible for arbitrary dimensions. If we assume this is possible for arbitrary dimensions, this would boost the success probability significantly. Thus, we also give an upper bound for the success probability of this protocol.

If the photons can be measured by all detectors, the projection looks like:

$$\begin{aligned}\langle P|_{abx_0x_1\ldots x_{N-3}} &= \langle 0|_{d_0}\langle 1|_{d_1}\ldots\langle N-1|_{d_{N-1}}\,\mathrm{QFT} \\ &= \frac{1}{\sqrt{N^N}}\sum_{\{i_0,i_1,\ldots,i_{N-1}\}\in P[N]}\omega^{\sum_{j=0}^{N-1} i_j d_j}\langle i_0 i_1\ldots i_{N-1}|_{abx_0x_1\ldots x_{N-3}}\quad .\end{aligned} \tag{4.14}$$

We see that the interferometer selects the modes (in the basis before the interferometer) with all photons in different time-bins: there are $N!$ modes that lead to success. The state Eq. (4.4) before the interferometer is a superposition of all combinations of time-bins: there are N^N input modes. Thus, the probability to be in a mode that leads to success is:

$$p_{\text{succ, up}} = \frac{N!}{N^N}\quad . \tag{4.15}$$

This is a much better scaling with dimension than the lower bound from Eq. (4.13). We give a few values for the lower and upper bound of the success probability in Table 4.1.

dimension N	3	4	5	6
$p_{\text{suc, low}}$	4.1×10^{-3}	6.1×10^{-5}	5.1×10^{-7}	2.8×10^{-9}
$p_{\text{suc, up}}$	$2/9$ (0.22)	$3/32$ (0.09)	$24/625$ (0.04)	$5/324$ (0.02)

Table 4.1: Lower and upper bound for the success probability of N-dimensional entanglement generation with the all-input modes protocol, calculated from Eq. (4.13) and (4.15) respectively.

Even if the upper bound of the success probability can be achieved for all dimensions, the success probability still decreases exponentially with dimension. In the next chapter, we propose a completely new protocol that achieves a polynomial scaling for even dimensions.

4.4. Implementation of the Quantum Fourier Transform with Linear Optical Elements

The quantum Fourier transform that we need in the all-input modes protocol as given by Eq. (4.5) can be described by an N x N unitary matrix. Reck and Zeilinger [41] showed in 1994 that any NxN unitary matrix can be decomposed in a sequence of two-dimensional unitary matrices. The two-dimensional matrices can be constructed with at most one beam splitter and one phase shifter. The number of beam splitters and phase shifters combinations scales with the dimension as $\frac{N(N+2)}{2}$ for an N-dimensional quantum Fourier transform. Barak and Ben-Aryeh [3] published a protocol that implements the N-dimensional quantum Fourier transform for $N=2^d$ with at most $d\cdot 2^{d-1}$ beam splitter and phase shifter combinations. Finally, Oshima [37] shows that the reduction of number of beam splitter and phase shifter combinations of Barek and Ben Aryeh holds for general dimensions where $N\neq$ prime. Thus, for all dimensions where $N\neq$ prime, the quantum Fourier transform can be implemented on the spatial modes with at most $d\cdot 2^{d-1}$ beam splitter and phase shifter combinations.

4.5. General Algorithm to Create Photon-Qudit Entanglement

We propose a general method to create the initial entanglement from Eq. (4.2) between Alice and Bob's energy levels with photonic qudits a and b respectively. Our implementation uses a quantum emitter coupled to a quantum memory with N energy levels, for example an NV center coupled to surrounding carbon atoms [47]. We find an overview of the system in Figure 4.2.

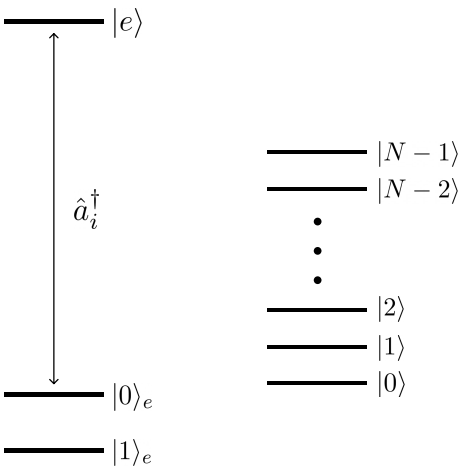

Figure 4.2: A quantum emitter on the left: the dark state $|1\rangle_e$ and the bright state $|0\rangle_e$ that can be excited to $|e\rangle$ and decay under emission of a photon in time-bin i. The quantum emitter is coupled to a quantum memory on the right with N energy levels.

There is an optical connection between $|0\rangle_e$ and $|e\rangle$: we can drive from $|0\rangle_e$ to the excited state $|e\rangle$ and the excited state will decay to the same ground state while emitting a photon. Aside from the electron spin, we need to interact with N energy levels in the qudit register. These are the energy levels Alice and Bob eventually want to entangle. We assume that it is possible to apply a controlled-NOT gate from each of these energy levels to the electron spin. Alice and Bob both execute the following protocol to generate qudit-photon entanglement:

Algorithm 1 Generating qudit-photon entanglement

1. Alice and Bob start in a superposition of all qudit levels and the electron spin starts in the level that is not optically active $|1\rangle_e$:

$$\frac{1}{\sqrt{N}} \sum_{k=0}^{N-1} |k\rangle \otimes |1\rangle_e \quad . \tag{4.16}$$

for $j \in \{0, 1, ..., d-1\}$ **do**

2. Alice and Bob apply a controlled-NOT operation with energy level $|j\rangle$ in the qudit register as control to the target qubit, the quantum emitter. The state after the first iteration ($j = 0$) is:

$$\frac{1}{\sqrt{N}} \left(\sum_{k=1}^{N-1} |k\rangle \otimes |1\rangle_e + |0\rangle \otimes |0\rangle_e \right) \quad . \tag{4.17}$$

3. Apply an optical pulse such that the optically active ground state $|0\rangle_e$ of the electron spin is excited to $|e\rangle$. The electron decays radiatively to $|0\rangle_e$ again and the corresponding photon is in time-bin j. Thus, the state from Eq. (4.17) becomes:

$$\frac{1}{\sqrt{N}} \left(\sum_{k=1}^{N-1} |k\rangle \otimes |1\rangle_e + |0\rangle \otimes |0\rangle_e \otimes |0\rangle_{ph} \right) \quad . \tag{4.18}$$

Here, $|j\rangle_{ph}$ indicates a photons in the j-th time-bin. We see that a photon is only emitted when the qudit register is in mode $|j\rangle$.

4. Alice and Bob apply the same controlled-NOT operation from step 2 again to flip the state of the quantum emitter to the dark state $|1\rangle_e$. In the first iteration $j = 0$, the state from Eq. (4.18) becomes:

$$\frac{1}{\sqrt{N}} \left(\sum_{k=1}^{N-1} |k\rangle \otimes |1\rangle_e + |0\rangle \otimes |1\rangle_e \otimes |0\rangle_{ph} \right) \quad . \tag{4.19}$$

end for

5. Now, Alice and Bob both have a state of the form:

$$\frac{1}{\sqrt{N}} \sum_{j=0}^{N-1} |j\rangle \otimes |1\rangle_e \otimes |j\rangle_{ph} \quad . \tag{4.20}$$

In the rest of the protocol, the state of the quantum emitter can be ignored since it is not entangled with the qudit register or the photonic qudit.

4.6. Algorithm to Create Photon-Qudit Entanglement with π-pulses

In the previous section, we discussed how to generate the initial states from Eq. (4.2) with multi-controlled operations. Some physical systems may have control over the energy levels in the quantum register in a way that allows us to generate the state in a simpler way. For example, if π - pulses can be applied between the electron spin and each energy level of the qudit register, the scheme from Figure 4.3 can be used:

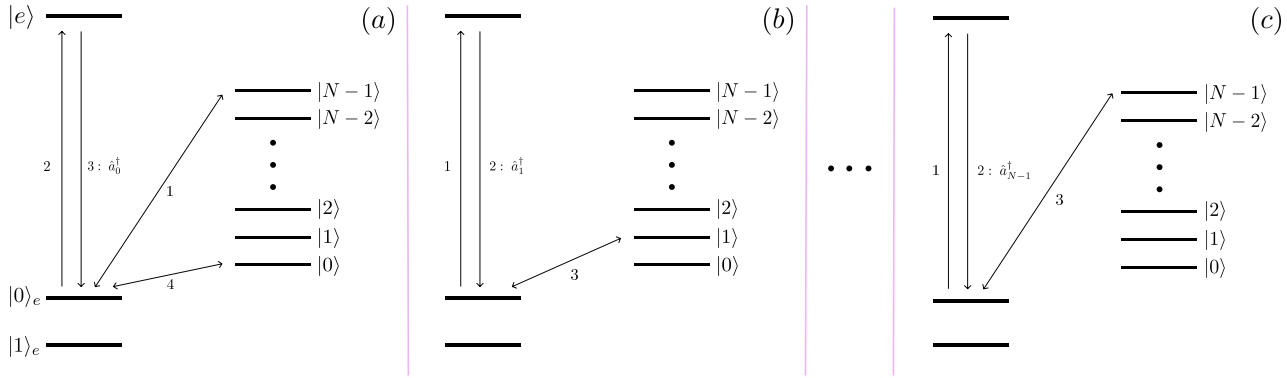

Figure 4.3: Creating the photon-qudit entanglement for the initial states from Eq. (4.2) with π-pulses, a quantum emitter and the qudit register.

Each energy level gets 'swapped' with the optically active electron ground state in subsequent time-bins by applying a π-pulse between an energy level and $|0\rangle_e$. After each π-pulse, the emitter is excited and a photon in that time-bin is emitted. By starting in a superposition of all energy levels in the qudit register, one photon entangled with all qudit levels is emitted. We describe the protocol in more detail in Algorithm 2.

Algorithm 2 Generating qudit-photon entanglement with π-pulses

1. Alice and Bob start in a superposition of all qudit levels and the electron spin starts in an arbitrary state:

$$\frac{1}{\sqrt{N}}\sum_{k=0}^{N-1}|k\rangle\otimes(\alpha\,|0\rangle_e+\beta\,|1\rangle_e)\ . \tag{4.21}$$

2. As we see in (a) of Figure 4.3, in step1. Alice and Bob apply a π-pulse between $|N-1\rangle$ and $|0\rangle_e$:

$$\left(\frac{1}{\sqrt{N}}\sum_{k=0}^{N-2}|k\rangle+\alpha\,|N-1\rangle\right)\otimes\left(\frac{1}{\sqrt{N}}\,|0\rangle_e+\beta\,|1\rangle_e\right)\ . \tag{4.22}$$

In step 2. they excite the quantum emitter from $|0\rangle_e$ to $|e\rangle$; in step 3. the emitter decays radiatively back to $|0\rangle_e$ and emits a photon in the 0-th time-bin:

$$\left(\frac{1}{\sqrt{N}}\sum_{k=0}^{N-2}|k\rangle+\alpha\,|N-1\rangle\right)\otimes\left(\frac{1}{\sqrt{N}}\,|0\rangle_e\otimes|0\rangle_{ph}+\beta\,|1\rangle_e\right)\ . \tag{4.23}$$

In step 4. they apply another π-pulse between $|0\rangle_e$ and $|0\rangle$. The resulting state is:

$$\left(\frac{1}{\sqrt{N}}\sum_{k=1}^{N-2}|k\rangle+\frac{1}{\sqrt{N}}\,|0\rangle\otimes|0\rangle_{ph}+\alpha\,|N-1\rangle\right)\otimes\left(\frac{1}{\sqrt{N}}\,|0\rangle_e+\beta\,|1\rangle_e\right)\ . \tag{4.24}$$

for $j\in\{0,1,...,d-1\}$ **do**

3. As we see in (b) and (c) of Figure 4.3, in step 1. Alice and Bob optically excite the emitter; in step 2. the emitter decays radiatively back to $|0\rangle_e$ and emits a photon in the j-th time-bin. For the first iteration ($j=1$), Eq. (4.24) becomes:

$$\left(\frac{1}{\sqrt{N}}\sum_{k=1}^{N-2}|k\rangle+\frac{1}{\sqrt{N}}\,|0\rangle\otimes|0\rangle_{ph}+\alpha\,|N-1\rangle\right)\otimes\left(\frac{1}{\sqrt{N}}\,|0\rangle_e\otimes|1\rangle_{ph}+\beta\,|1\rangle_e\right)\ . \tag{4.25}$$

In step 3. they apply a π-pulse between $|0\rangle_e$ and energy level $|j\rangle$ from the qudit register:

$$\left(\frac{1}{\sqrt{N}}\left(\sum_{k=2}^{N-2}|k\rangle+|0\rangle\otimes|0\rangle_{ph}+|1\rangle\otimes|1\rangle_{ph}\right)+\alpha\,|N-1\rangle\right)\otimes\left(\frac{1}{\sqrt{N}}\,|0\rangle_e+\beta\,|1\rangle_e\right)\ . \tag{4.26}$$

end for

4. After all iterations of the for-loop, Alice and Bob both have the following state:

$$\frac{1}{\sqrt{N}}\sum_{k=0}^{N-1}|k\rangle\,|k\rangle_{ph}\otimes(\alpha\,|0\rangle_e+\beta\,|1\rangle_e)\ . \tag{4.27}$$

In the rest of the protocol, the state of the quantum emitter can be ignored since it is not entangled with the qudit register or the photonic qudit.

5

N-Dimensional Entanglement Protocol with Tailored Ancilla Photons

The previous all-input modes protocol demonstrates an implementation of the Bell state measurement as proposed by Luo et al. [32] for time-bin encoded photonic qudits instead of spatially encoded photons. In this section, we propose a completely new protocol for the generation of high dimensional entanglement in even dimensions: we call this the tailored protocol. The difference lies in the state preparation of the ancillary photons. The previous protocol uses an equal superposition of all modes for the ancillary state. We tailor the state of the ancillary photons to the modes that the quantum Fourier transform can choose, such that the photons from Alice and Bob are projected into an N-dimensional state. This increases the probability of success to a polynomial scaling with dimension, which is an exponential speed-up with respect to the previous protocol. To better illustrate this concept, we consider the generation of 4-dimensional entanglement with our protocol in Section 5.2. We also investigate the analytical expression for the success probability in Section 5.4 and show why our protocol does not work for odd dimensions in Section 5.5. First, we start with a description of our protocol.

5.1. Description of the Protocol

Alice and Bob want to entangle their qudit registers that consist of N energy levels. Here N needs to be even, but not necessarily a power of 2. If $N = 2^d, d \in \mathscr{R}$, the state shared by Alice and Bob in case of success can be written as d Bell pairs. They execute the following steps:

1. Alice and Bob start with a superposition of their N energy levels:

$$|\psi\rangle = \frac{1}{\sqrt{N}} \sum_{k=0}^{N-1} |k\rangle \quad . \tag{5.1}$$

2. Entangle each mode $|k\rangle$ with the presence of a photon in the k-th time-bin as described in Section 4.5 and 4.6:

$$|\psi\rangle_{\text{in}} = \frac{1}{\sqrt{N}} \sum_{k=0}^{N-1} |k\rangle\,|k\rangle_{ph} \quad . \tag{5.2}$$

3. The $N-2$ ancillary photons are prepared in the entangled state from Eq. (5.14) according to the protocol described in Section 5.6.
4. The photons from Alice and Bob and $N-2$ ancillary photons go to a middle station where they undergo a Bell state measurement. The Bell state measurement is implemented with an N-dimensional quantum Fourier transform as described in Section 4.4 and N photon detectors.

5. The middle station classically sends the detection pattern to Alice and Bob.
6. If all photons are measured in different time-bins, the time-bin information has been removed the protocol has succeeded. In this case, either Alice or Bob applies the outcome-dependent local unitary operation $U(d_0, d_1, ..., d_{N-1})$ from Eq. (5.19). Otherwise, the protocol is repeated.

The high-level scheme is the same as in the all-modes protocol so the overview in Figure 4.1 is also relevant here.

5.2. Generating 4-Dimensional Entanglement

Before we go to the proof in arbitrary dimensions we consider an example in 4 dimensions. We show the set-up in Figure 5.1. Alice and Bob both have two qubits that they want to entangle simultaneously. Together with two ancillary photons x_0 and x_1 they arrive at the middle station. The quantum Fourier transform is implemented with 4 beam splitters and one phase shifter. Afterwards, the photons are measured by photon detectors $0, 1, 2, 3$.

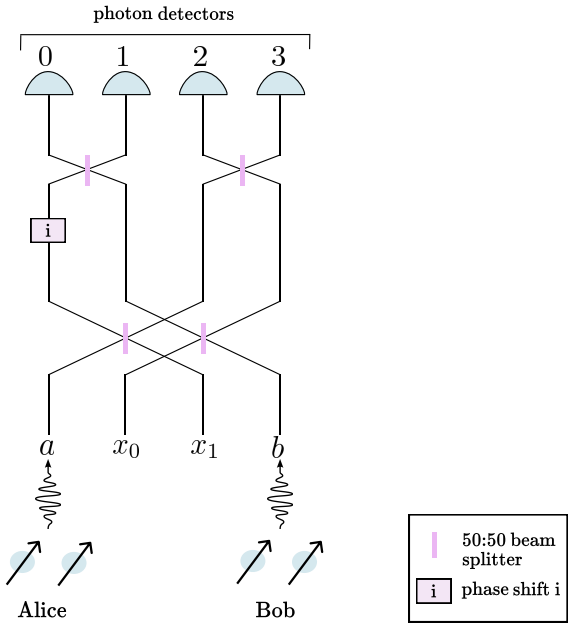

Figure 5.1: Generating 4-dimensional entanglement, or equivalently two Bell pairs, between Alice and Bob with the tailored protocol. The quantum Fourier transform is implemented with 4 beam splitters and a phase shifter.

Alice and Bob start with step 1: they both entangle the four modes of their qubits with a photonic qudit in four time-bins:

$$|\psi\rangle = \frac{1}{2}\left(|00\rangle|0\rangle + |01\rangle|1\rangle + |10\rangle|2\rangle + |11\rangle|3\rangle\right) \quad . \tag{5.3}$$

Every first ket $|i'\rangle$ corresponds to the two-qubit state written in binary and the second ket $|i\rangle$ corresponds to a photon in the i-th time-bin. Since our goal is to achieve four-dimensional entanglement, the Schmidt rank of the final state is $S = 4$. According to the proof of Calsamiglia [12] we need four initial particles as we also see in Figure 5.1. We already have two photons coming from Alice and Bob, so we need two ancillary photons x_0 and x_1.

From Eq. (5.14) we see that there are multiple states to choose for the ancillary photons. For the sake of this example, we choose the following state:

$$|\text{anc}\rangle = \frac{1}{\sqrt{2}}\left(|01\rangle_{x_0x_1} + |23\rangle_{x_0x_1}\right) \ . \tag{5.4}$$

$$\begin{aligned}|\psi\rangle_{ABabx_0x_1} = \frac{1}{\sqrt{2}\cdot 4}\Big(|00\rangle_A|0\rangle_a + |01\rangle_A|1\rangle_a + |10\rangle_A|2\rangle_a + |11\rangle_A|3\rangle_a\Big) \otimes \Big(|00\rangle_B|0\rangle_b + |01\rangle_B|1\rangle_b + |10\rangle_B|2\rangle_b + |11\rangle_B|3\rangle_b\Big) \\ \otimes \Big(|01\rangle_{x_0x_1} + |23\rangle_{x_0x_1}\Big) \ .\end{aligned} \tag{5.5}$$

Here, we indicate Alice and Bob's spin qubits with subscript A and B, the photons from Alice and Bob's side with a and b and the ancillary photons with x_0 and x_1. The protocol succeeds if all photons are measured in different time-bins and it does not matter at which detector these photons are measured. Thus, we write the projection of photons a, b, x_0 and x_1 in terms of $(d_1, d_2, d_3, d_4) \in \{0,1,2,3\}^4$ where each d_i corresponds to the output port at which a photon in time-bin i is measured. We apply the quantum Fourier transform to the photon detections and we arrive at a useful expression in the basis before the interferometer:

$$\begin{aligned}\langle P|_{abx_0x_1} &= \langle 0|_{d_1}\langle 1|_{d_2}\langle 2|_{d_3}\langle 3|_{d_4}\,\text{QFT} \\ &= \frac{1}{2^4}\Big(\langle 0|_a + \omega^{d_1}\langle 0|_b + \omega^{2d_1}\langle 0|_{x_1} + \omega^{3d_1}\langle 0|_{x_2}\Big) \otimes \Big(\langle 1|_a + \omega^{d_2}\langle 1|_b + \omega^{2d_2}\langle 1|_{x_1} + \omega^{3d_2}\langle 1|_{x_2}\Big) \\ &\otimes \Big(\langle 2|_a + \omega^{d_3}\langle 2|_b + \omega^{2d_3}\langle 2|_{x_1} + \omega^{3d_3}\langle 2|_{x_2}\Big) \otimes \Big(\langle 3|_a + \omega^{d_4}\langle 3|_b + \omega^{2d_4}\langle 3|_{x_1} + \omega^{3d_4}\langle 3|_{x_2}\Big) \\ &= \frac{1}{2^4}\Big(\omega^{d_2+2d_3+3d_4}\langle 0123| + \omega^{d_2+2d_4+3d_3}\langle 0132| + \omega^{d_3+2d_2+3d_4}\langle 0213| + \omega^{d_3+2d_4+3d_2}\langle 0231| + \omega^{d_4+2d_2+3d_3}\langle 0312| \\ &+ \omega^{d_4+2d_3+3d_2}\langle 0321| + \omega^{d_1+2d_3+3d_4}\langle 1023| + \omega^{d_1+2d_4+3d_3}\langle 1032| + \omega^{d_3+2d_1+3d_4}\langle 1203| + \omega^{d_3+2d_4+3d_1}\langle 1230| \\ &+ \omega^{d_4+2d_1+3d_3}\langle 1302| + \omega^{d_4+2d_3+3d_1}\langle 1320| + \omega^{d_1+2d_2+3d_4}\langle 2013| + \omega^{d_1+2d_4+3d_2}\langle 2031| + \omega^{d_2+2d_1+3d_4}\langle 2103| \\ &+ \omega^{d_2+2d_4+3d_1}\langle 2130| + \omega^{d_4+2d_1+3d_2}\langle 2301| + \omega^{d_4+2d_2+3d_1}\langle 2310| + \omega^{d_1+2d_2+3d_3}\langle 3012| + \omega^{d_1+2d_3+3d_2}\langle 3021| \\ &+ \omega^{d_2+2d_1+3d_3}\langle 3102| + \omega^{d_2+2d_3+3d_1}\langle 3120| + \omega^{d_3+2d_1+3d_2}\langle 3201| + \omega^{d_3+2d_2+3d_1}\langle 3210|\Big)_{abx_0x_1} \ .\end{aligned} \tag{5.6}$$

Here, we only keep the terms that are physically possible in our protocol: a, b, x_0 and x_1 all correspond to exactly one photon, so we neglect the terms that don't satisfy this condition. Now we consider the ancillary photons as part of the Bell state measurement by applying the projection of Eq. (5.6) to the state of the ancillary photons. We find the projection of the photons coming from Alice and Bob $\langle P|_{ab}$:

$$\langle P|_{ab} = \langle P|_{abx_0x_1}|\text{anc}\rangle = \frac{1}{\sqrt{2}\cdot 2^6}\Big(\omega^{d_4+2d_1+3d_2}\langle 23|_{ab} + \omega^{d_3+2d_1+3d_2}\langle 32|_{ab} + \omega^{d_2+2d_3+3d_4}\langle 01|_{ab} + \omega^{d_1+2d_3+3d_4}\langle 10|_{ab}\Big) \ . \tag{5.7}$$

The modes in the projection from Eq. (5.6) contains all permutations of the time-bins. Thus, each mode $|ij\rangle_{x_1x_2}$ in the ancilla state yields two non-zero terms in the projection from Eq. (5.7): $\langle kl|_{ab}$ and $\langle lk|_{ab}$ where $i \neq j \neq k \neq l$.

Finally, we apply the projection from Eq. (5.7) to the state of Alice and Bob's qubits and photons from Eq. (5.5) to find the state of the spin qubits:

$$\begin{aligned}|\psi\rangle_{out} = \langle P|_{ab}|\psi\rangle_{ABab} = \frac{1}{\sqrt{2}\cdot 2^6}\Big(&\omega^{d_4+2d_1+3d_2}|10\rangle_A|11\rangle_B + \omega^{d_3+2d_1+3d_2}|11\rangle_A|10\rangle_B \\ &+ \omega^{d_2+2d_3+3d_4}|00\rangle_A|01\rangle_B + \omega^{d_1+2d_3+3d_4}|01\rangle_A|00\rangle_B\Big) \ .\end{aligned} \tag{5.8}$$

This is almost the entangled state we want except for the phases in front of the modes. These phases are defined by the output ports where the photons are detected. Thus, we can apply the following unitary $U(d_1,d_2,d_3,d_4)$ on either Alice's qubits or Bob's qubits conditional on the corresponding output ports:

$$U(d_1,d_2,d_3,d_4) = \omega^{-d_1-2d_3-3d_4}|00\rangle\langle 00| + \omega^{-d_2-2d_3-3d_4}|01\rangle\langle 01| + \omega^{-d_3-2d_1-3d_2}|10\rangle\langle 10| + \omega^{-d_4-2d_1-3d_2}|11\rangle\langle 11| \ . \tag{5.9}$$

We arrive at the final Bell state:

$$\begin{aligned} |\Psi\rangle_{4D} &= I^A \otimes U^B(d_1,d_2,d_3,d_4)\,|\psi\rangle_{out} = \frac{1}{\sqrt{2}\cdot 2^6}\left(|10\rangle_A|11\rangle_B + |11\rangle_A|10\rangle_B + |00\rangle_A|01\rangle_B + |01\rangle_A|00\rangle_B\right) \\ &= \frac{1}{\sqrt{2}\cdot 2^5}\left(\frac{1}{2}(|00\rangle_{AB}+|11\rangle_{AB})\otimes(|01\rangle_{AB}+|10\rangle_{AB})\right) \ . \end{aligned} \tag{5.10}$$

Here, the subscript $4D$ indicates a four-dimensional Bell state and we chose to apply the unitary operation on Bob's side. The Bell state can be written as the product of two two-dimensional Bell states and we have successfully created two entangled pairs simultaneously.

Success Probability

We calculate the success probability of one successful detection pattern by squaring the constant in front of the two Bell states from Eq. (5.10): $p_1 = \left|\frac{1}{\sqrt{2}\cdot 2^5}\right|^2$. The unitary operation from Eq. (5.9) can be applied for all combinations of output ports that click, the only requirement is that the photons are in all-different time-bins. Thus, the number of successful detection patterns is 4^4 and each successful detection pattern occurs with the same probability p_1. The total probability of success for this protocol in four dimensions is:

$$p_{succ} = \left|\frac{1}{\sqrt{2}\cdot 2^5}\right|^2 \cdot 4^4 = \frac{1}{2^3} \ . \tag{5.11}$$

5.3. Proof for Arbitrary Even Dimensions

In this section we present the proof of our protocol and in the next section we will consider the four-dimensional case. The aim of the protocol is to herald an N-dimensional entangled state $|\Psi\rangle_{\mathrm{ND}}$ between Alice and Bob:

$$\begin{aligned} |\Psi\rangle_{\mathrm{ND}} &= \frac{1}{\sqrt{N}}\sum_{j=0}^{\frac{N}{2}-1}\left(|c_j b_j\rangle_{AB} + |b_j c_j\rangle_{AB}\right) \\ &(c_j,b_j) \in \{0,1,...,N-1\}^2 \ \wedge \ c_i \neq c_j \neq b_i \neq b_j \ \forall\, i,j \ . \end{aligned} \tag{5.12}$$

This state does not describe all high-dimensional entangled states but we use this notation since it is the output state of our protocol, as we will see later on. Alice and Bob start with the following state:

$$\begin{aligned} |\psi\rangle_{ABab} &= \frac{1}{\sqrt{N}}\sum_{i=0}^{N-1}|i\rangle_A|i\rangle_a \otimes \frac{1}{\sqrt{N}}\sum_{k=0}^{N-1}|k\rangle_B|k\rangle_b \\ &= \frac{1}{N}\sum_{i=0}^{N-1}\sum_{k=0}^{N-1}|i\rangle_A|i\rangle_a|k\rangle_B|k\rangle_b \ . \end{aligned} \tag{5.13}$$

Here, we indicate the state of Alice's qudit with subscript A, the state of Bob's qudit with B and the photonic qudits are denoted by a and b. In the all-input modes protocol the state of the ancillary photons

is an equal superposition state before the Bell state measurement. In the tailored protocol, the $N-2$ ancillary photons $x_0, x_1, ..., x_{N-1}$ are in the following state:

$$|\text{anc}\rangle = \frac{1}{\sqrt{N/2}} \sum_{j=0}^{\frac{N}{2}-1} |a_{j,0} a_{j,1} \dots a_{j,N-3}\rangle_{x_0 x_1 \dots x_{N-3}} \quad . \tag{5.14}$$

with the following constraints:

$$\begin{aligned} &(a_{j,0}, a_{j,1}, ..., a_{j,N-3}) \in P[0,1,...,N-1] \\ &a_{j,0}, a_{j,1}, ..., a_{j,N-4} \neq c_j, b_j \\ &(c_j, b_j) \in \{0,1,...,N-1\}^2 \\ &c_i \neq b_j \neq c_j \neq b_i \quad \forall\, i,j \ . \end{aligned} \tag{5.15}$$

Here, the index that we sum over appears in the third constraint as well. Each mode is a permutation of all time-bins except for two time-bins. In each mode two time-bins are excluded and the choice for these two time-bins is unique for each mode. Also, the two time-bins excluded in one mode need to be different. We see later that the c_j and b_j eventually form the high-dimensional state Eq. (5.12). Note that in the all-input modes protocol of Chapter 4 the state is a superposition of $N^{(N-2)/2}$ terms, while we only have $\frac{N}{2}$ terms here.

The Bell state measurement is applied with the quantum Fourier transform in N dimensions. After the Bell state measurement, the photons have become indistinguishable and we measure them with N photon detectors. The condition for success is to measure the photons in all different time-bins. We look at the projection of N photons in different time-bins and apply the quantum Fourier transform to get an expression in the basis before the Bell state measurement:

$$\begin{gathered} \langle P| = \langle 0|_{d_0} \langle 1|_{d_1} \dots \langle N|_{d_{N-1}} \,\text{QFT} = \frac{1}{N^{N/2}} \sum_{t_0=0}^{N-1} \sum_{t_1=0}^{N-1} \dots \sum_{t_{N-1}=0}^{N-1} \omega^{\sum_{i=0}^{N-1} t_i d_i} \langle t_0 t_1 \dots t_{N-1}|_{a b x_0 x_1 \dots x_{N-1}} \\ \text{for } (t_0, t_1, ..., t_{N-1}) \in P[0,1,...,N-1] \ . \end{gathered} \tag{5.16}$$

Again, d_i represents the number of the output port at which a photon in time-bin i is measured. This expression holds for every possible detection pattern where the photons are measured in different time-bins. The projection describes the sum of all permutations of photons in different time-bins and each permutation has a unique phase in front. Here ω is defined as: $\omega = e^{\frac{2\pi i}{N}}$.

We consider the ancillary photons as part of the interferometer by applying the projection to the ancillary photons and we are left with the projection of the photons a and b.

$$\langle P|_{ab} = \langle P|\text{anc}\rangle = \frac{1}{\sqrt{N^N} \cdot \sqrt{\frac{N}{2}}} \sum_{j=0}^{\frac{N}{2}-1} \omega^{a_{j,0} d_2 + a_{j,1} d_3 + \dots + a_{j,N-3} d_{N-1}} \left(\omega^{c_j d_0 + b_j d_1} \langle c_j b_j|_{ab} + \omega^{b_j d_0 + c_j d_1} \langle b_j c_j|_{ab} \right) \ . \tag{5.17}$$

Here the $a_{j,i}$ correspond to the terms in the state of the ancillary photons that we chose, so they are known to us. By excluding two time-bins in the ancillary state Eq. (5.14), we are able to tailor the projection of the photons coming from Alice and Bob such that we project into orthogonal modes. We finally arrive at the output state of Alice and Bob by applying Eq. (5.17) to the state of Alice and Bob and their photons Eq. (5.13):

$$|\psi\rangle_{AB}^{\text{out}} = \langle P|_{ab}\,|\psi\rangle_{ABab} = \frac{1}{\sqrt{N^N}\cdot\sqrt{\frac{N}{2}}\cdot N}\sum_{j=0}^{\frac{N}{2}-1}\omega^{a_{j,0}d_2+a_{j,1}d_3+\ldots+a_{j,N-3}d_{N-1}}\left(\omega^{c_jd_0+b_jd_1}\,|c_jb_j\rangle_{AB}+\omega^{b_jd_0+c_jd_1}\,|b_jc_j\rangle_{AB}\right)$$
$$= \frac{\sqrt{N}}{\sqrt{N^N}\cdot\sqrt{\frac{N}{2}}\cdot N}\sum_{j=0}^{\frac{N}{2}-1}\omega^{a_{j,0}d_2+a_{j,1}d_3+\ldots+a_{j,N-3}d_{N-1}}\left(\frac{\omega^{c_jd_0+b_jd_1}}{\sqrt{N}}\,|c_jb_j\rangle_{AB}+\frac{\omega^{b_jd_0+c_jd_1}}{\sqrt{N}}\,|b_jc_j\rangle_{AB}\right)\ . \tag{5.18}$$

The state $|\psi\rangle_{AB}^{\text{out}}$ consists of the modes that we want in our final state but they still have phases. To get rid of the phases, we apply the following unitary on Bob's side:

$$U(d_0,d_1,\ldots,d_{N-1}) = \sum_{j=0}^{N/2-1}\omega^{-\sum_{i=0}^{N-3}a_{j,i}d_{i+2}}\left(\omega^{-c_jd_0-b_jd_1}\,|b_j\rangle\langle b_j| + \omega^{-b_jd_0-c_jd_1}\,|c_j\rangle\langle c_j|\right)\ . \tag{5.19}$$

It does not matter if Alice or Bob applies the unitary operation but the expression of $U(d_0,d_1,\ldots,d_{N-1})$ will be slightly different if we apply it on Alice's side: the b_j and c_j are switched in the bras and kets. By applying the unitary operation we go to:

$$|\Psi\rangle_{ND} = \frac{1}{\sqrt{N}}\sum_{j=0}^{\frac{N}{2}-1}\left(|c_jb_j\rangle+|b_jc_j\rangle\right)$$
$$\text{for } (c_j,b_j)\in\{0,1,\ldots,N-1\}^2\ \wedge\ c_i\neq c_j\neq b_i\neq b_j\ \ \forall\ i,j\ . \tag{5.20}$$

Alice and Bob have arrived at an N-dimensional entangled state!

5.4. Success Probability

The probability of one successful detection pattern is the square of the constant from Eq. (5.18): $\left|\frac{\sqrt{N}}{\sqrt{N^N}\sqrt{\frac{N}{2}}\cdot N}\right|^2$. We have shown that the combination of output ports that click does not matter, thus each photon can be detected in each of the N output ports. Since there are N photons, this leads to N^N successful detection patterns. The total success probability scales with dimension as

$$p_{\text{succ}} = \left|\frac{\sqrt{N}}{\sqrt{N^N}\sqrt{\frac{N}{2}}\cdot N}\right|^2\cdot N^N = \frac{2}{N^2}\ . \tag{5.21}$$

5.5. Example for Odd Dimensions

To show that our protocol does not create a high-dimensional state for odd dimensions, we consider the case where $N=5$. The Schmidt rank of the state $|\Psi\rangle_{5D}$ we want is $S=5$. This state could look like:

$$|\Psi\rangle_{5D} = \frac{1}{\sqrt{5}}\left(|00\rangle+|11\rangle+|22\rangle+|33\rangle+|44\rangle\right)_{AB}\ . \tag{5.22}$$

According to Calsamiglia's theorem [12] we need at least 5 initial particles. Since we have two photons coming from Alice and Bob, we need three ancillary photons. The joint state of Alice, Bob and their photons a and b looks like:

$$|\psi\rangle_{ABab} = \frac{1}{5}\left(|0\rangle_A|0\rangle_a+|1\rangle_A|1\rangle_a+|2\rangle_A|2\rangle_a+|3\rangle_A|3\rangle_a+|4\rangle_A|4\rangle_a\right)$$
$$\otimes\left(|0\rangle_B|0\rangle_b+|1\rangle_B|1\rangle_b+|2\rangle_B|2\rangle_b+|3\rangle_B|3\rangle_b+|4\rangle_B|4\rangle_b\right)\ . \tag{5.23}$$

The projection of the 5 photons in all different time-bins in the basis before the interferometer is:

$$\begin{aligned}\langle P| &= \langle 0|_{d_0} \langle 1|_{d_1} \langle 2|_{d_2} \langle 3|_{d_3} \langle 4|_{d_4} \,\mathrm{QFT} \\ &= \frac{1}{\sqrt{5^5}} \sum_{t_0=0}^{N-1} \sum_{t_1=0}^{N-1} \cdots \sum_{t_4=0}^{N-1} \omega^{t_0 d_0 + t_1 d_1 + t_2 d_2 + t_3 d_3 + t_4 d_4} \langle t_0 t_1 ... t_4| \\ &\text{for } (t_0, t_1, ..., t_4) \in P[0,1,2,3,4] \ .\end{aligned} \tag{5.24}$$

Here, $(d_0, d_1, ..., d_4) \in \{0,1,2,3,4\}^5$ where the $0,1,2,3,4$ correspond to the output ports. All combinations of output ports are possible here as long as all photons are measured in different time-bins. The time-bins correspond to t_i. To execute the tailored protocol, we should prepare the ancilla photons in the state:

$$\begin{aligned}|\mathrm{anc}\rangle = \frac{1}{\sqrt{3}} &(|a_{0,0} a_{0,1} a_{0,2}\rangle + |a_{1,0} a_{1,1} a_{1,2}\rangle + |a_{2,0} a_{2,1} a_{2,2}\rangle) \\ &\text{for } \{a_{i,0}, a_{i,1}, a_{i,3}\} \in P[0,1,2,3,4] \ \forall \ i = 0,1,2 \\ &\wedge \ a_{0,0}, a_{0,1}, a_{0,2} \neq b_0, c_0 \\ &\wedge \ a_{1,0}, a_{1,1}, a_{1,2} \neq b_1, c_1 \\ &\wedge \ a_{2,0}, a_{2,1}, a_{2,2} \neq b_2, c_2 \\ &\wedge \ \{b_0, c_0, b_1, c_1, b_2\} \in P[0,1,2,3,4] \ .\end{aligned} \tag{5.25}$$

From Section 5.3 we know that each mode should contain a permutation of three time-bins and exclude two time-bins. The time-bins that are excluded in each mode should be unique. However, since there are 5 time-bins and we need to exclude 6 time-bins that are not equal to each other (b_0, c_0, b_1, c_1, b_2 and c_2) this is not possible. Thus there is too much overlap in the modes since two exclusion parameters are the same.

Suppose c_2 is equal to b_0. We apply the projection of Eq. (5.24) to the state of the ancillary photons in Eq. (5.25) to find the projection of photons a and b:

$$\begin{aligned}\langle P|_{ab} = \langle P|\mathrm{anc}\rangle = \frac{1}{\sqrt{5^5}\sqrt{3}} \Big(&\omega^{b_0 d_0 + c_0 d_1 + a_{0,0} d_2 + a_{0,1} d_3 + a_{0,2} d_4} \langle b_0 c_0| + \omega^{c_0 d_0 + b_0 d_1 + a_{0,0} d_2 + a_{0,1} d_3 + a_{0,2} d_4} \langle c_0 b_0| \\ &+ \omega^{b_1 d_0 + c_1 d_1 + a_{1,0} d_2 + a_{1,1} d_3 + a_{1,2} d_4} \langle b_1 c_1| + \omega^{c_1 d_0 + b_1 d_1 + a_{1,0} d_2 + a_{1,1} d_3 + a_{1,2} d_4} \langle c_1 b_1| \\ &+ \omega^{b_2 d_0 + c_2 d_1 + a_{2,0} d_2 + a_{2,1} d_3 + a_{2,2} d_4} \langle b_2 c_2| + \omega^{c_2 d_0 + b_2 d_1 + a_{2,0} d_2 + a_{2,1} d_3 + a_{2,2} d_4} \langle c_2 b_2| \Big)_{ab} \ .\end{aligned} \tag{5.26}$$

Finally, we apply the above projection of a and b to the state Alice and Bob start with from Eq. (5.23):

$$\begin{aligned}\langle P_{ab}|\psi\rangle_{ABab} = \frac{1}{5 \cdot \sqrt{5^5}\sqrt{3}} \Big(&\omega^{b_0 d_0 + c_0 d_1 + a_{0,0} d_2 + a_{0,1} d_3 + a_{0,2} d_4} |b_0 c_0\rangle_{AB} + \omega^{c_0 d_0 + b_0 d_1 + a_{0,0} d_2 + a_{0,1} d_3 + a_{0,2} d_4} |c_0 b_0\rangle_{AB} \\ &+ \omega^{b_1 d_0 + c_1 d_1 + a_{1,0} d_2 + a_{1,1} d_3 + a_{1,2} d_4} |b_1 c_1\rangle_{AB} + \omega^{c_1 d_0 + b_1 d_1 + a_{1,0} d_2 + a_{1,1} d_3 + a_{1,2} d_4} |c_1 b_1\rangle_{AB} \\ &+ \omega^{b_2 d_0 + c_2 d_1 + a_{2,0} d_2 + a_{2,1} d_3 + a_{2,2} d_4} |b_2 c_2\rangle_{AB} + \omega^{c_2 d_0 + b_2 d_1 + a_{2,0} d_2 + a_{2,1} d_3 + a_{2,2} d_4} |c_2 b_2\rangle_{AB} \Big) \ .\end{aligned} \tag{5.27}$$

After applying the unitary operation $U(d_0, d_1, ..., d_4)$ as defined by Eq. (5.19), Alice and Bob share the

state:

$$
\begin{aligned}
|\Psi\rangle_{\text{out}} &= \frac{1}{5\cdot\sqrt{5^5}\sqrt{3}}\Big(|b_0c_0\rangle_{AB}+|c_0b_0\rangle_{AB}+|b_1c_1\rangle_{AB}+|c_1b_1\rangle_{AB}+|b_2c_2\rangle_{AB}+|c_2b_2\rangle_{AB}\Big)\\
&= \frac{1}{5\cdot\sqrt{5^5}\sqrt{3}}\Big(|b_0c_0\rangle_{AB}+|c_0b_0\rangle_{AB}+|b_1c_1\rangle_{AB}+|c_1b_1\rangle_{AB}+|b_2b_0\rangle_{AB}+|b_0b_2\rangle_{AB}\Big) \qquad (5.28)\\
&= \frac{1}{5\cdot\sqrt{5^5}\sqrt{3}}\Big(|b_0\rangle_A\otimes(|c_0\rangle+|b_2\rangle)_B+(|c_0\rangle+|b_2\rangle)_A\otimes|b_0\rangle_B+|b_1c_1\rangle_{AB}+|c_1b_1\rangle_{AB}\Big)\ .
\end{aligned}
$$

In the second step of the above calculation, we substitute b_0 for c_2 and we see that the Schmidt rank can at most be $S=4$. This extends to all odd dimensions N_{odd}: the protocol with entangled ancillary photons yields a state with Schmidt rank $S=N_{\text{odd}}-1$ instead of $S=N_{\text{odd}}$. Thus, the tailored protocol can not generate N_{odd}-dimensional entangled states.

5.6. Algorithm to Create the Tailored State

Executing the tailored protocol in N dimensions requires $N-2$ ancillary photons. To create the state of the ancillary photons from Eq. (5.14), we consider the 6-dimensional tailored protocol. We want the 4 ancillary photonic qudits to be in the state:

$$
|\text{anc}\rangle = \frac{1}{\sqrt{3}}\left(|0123\rangle+|2345\rangle+|4501\rangle\right)\ . \qquad (5.29)
$$

Here, in each mode $|i_0i_1i_2i_3\rangle$ the i_0,i_1,i_2,i_3 represent the time-bins of the photon and the position inside the ket represents the spatial mode $0,1,2,3$: each spatial mode contains one photon. We can choose other states for the ancillary photons, but for the sake of this example we choose this state. We do require that there is no overlap in the time-bins of all spatial modes. If we have two modes $|i_0i_1i_2i_3\rangle$ and $|i_4i_5i_6i_7\rangle$, we require that $i_0\neq i_4\ \wedge\ i_1\neq i_5\ \wedge\ i_2\neq i_6\ \wedge\ i_3\neq i_7$.

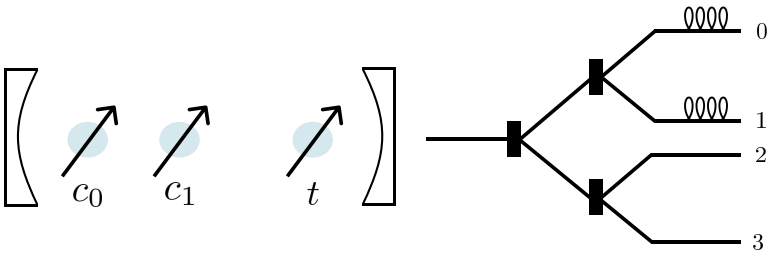

Figure 5.2: Creating the state of the ancillary photonic qudits for the 6-dimensional tailored protocol. Photons are emitted by exciting the target emitter controlled on qubits c_0 and c_1. Optical switches (black rectangles) route the photons to the correct spatial mode and the delay lines ensure that the photons are in the correct time-bins.

We start with two control qubits that we indicate with subscript c_0,c_1 and one target qubit t that is a quantum emitter with $|0\rangle$ as the optically active ground state as we visualize in Figure 5.2. Since we need a superposition of three modes, we start in the state:

$$
\frac{1}{\sqrt{3}}\left(|00\rangle+|01\rangle+|10\rangle\right)_{c_0c_1}\otimes|1\rangle_t\ . \qquad (5.30)
$$

Now we build up the state from Eq. (5.29) by applying bit flips to the quantum emitter, controlled by the modes of the control qubits.

After each controlled bit flip of the quantum emitter, we excite the quantum emitter such that it decays radiatively and apply the same controlled operation again to bring the quantum emitter back to the dark state $|1\rangle_t$. Since we use these steps often in the protocol below, let us call this the emission of a photon controlled on $|ij\rangle_{c_0c_1}$.

1. We first emit a photon controlled on mode $|00\rangle_{c_0c_1}$ We use an optical switch to route this photon to spatial mode 0. The joint state of the control qubits, target qubit and photons in spatial modes is:

$$\frac{1}{\sqrt{3}}\left(|00\rangle|0\mathrm{vvv}\rangle+|01\rangle|\mathrm{vvvv}\rangle+|10\rangle|\mathrm{vvvv}\rangle\right)_{c_0c_1}\otimes|1\rangle_t \quad . \tag{5.31}$$

   Here, $|v\rangle$ indicates the absence of photons in that spatial mode.
2. After time Δt we flip the quantum emitter controlled on $|10\rangle_{c_0c_1}$ and route the photon to spatial mode 3. Since spatial mode 0 is delayed by a delay loop with time Δt, the state is:

$$\frac{1}{\sqrt{3}}\left(|00\rangle|0\mathrm{vvv}\rangle+|01\rangle|\mathrm{vvvv}\rangle+|10\rangle|\mathrm{vv0v}\rangle\right)_{c_0c_1}\otimes|1\rangle_t \quad . \tag{5.32}$$

3. After time Δt we emit a photon controlled on mode $|01\rangle_{c_0c_1}$ and route this to spatial mode 0. Again after time Δt we emit a photon controlled on mode $|00\rangle_{c_0c_1}$ and route this to spatial mode 2. Since spatial mode 0 contains a delay loop, both emitted photons in this step are in the same time-bin 1 so the state is:

$$\frac{1}{\sqrt{3}}\left(|00\rangle|01\mathrm{vv}\rangle+|01\rangle|\mathrm{vvvv}\rangle+|10\rangle|\mathrm{vv01}\rangle\right)_{c_0c_1}\otimes|1\rangle_t \quad . \tag{5.33}$$

4. After time Δt we emit a photon controlled on mode $|01\rangle_{c_0c_1}$ and route this to spatial mode 0. Again after Δt we emit a photon controlled on $|00\rangle_{c_0c_1}$ and route this to spatial mode 3. Since spatial mode 0 is delayed by Δt, the state is:

$$\frac{1}{\sqrt{3}}\left(|00\rangle|012\mathrm{v}\rangle+|01\rangle|2\mathrm{vvv}\rangle+|10\rangle|\mathrm{vv01}\rangle\right)_{c_0c_1}\otimes|1\rangle_t \quad . \tag{5.34}$$

We continue to build up the ancillary state in this way until we arrive at:

$$\frac{1}{\sqrt{3}}\left(|00\rangle_{c_0c_1}|0123\rangle+|01\rangle_{c_0c_1}|2345\rangle+|10\rangle_{c_0c_1}|4501\rangle\right)\otimes|1\rangle_t \quad . \tag{5.35}$$

We can neglect the state of the target qubit since it is not entangled with the state of the photonic qudits. We measure the control qubits in the right basis to remove the entanglement with the photonic qudits. Finally we arrive at Eq. (5.29).

In general, to execute the N-dimensional tailored protocol, we need $N-2$ ancillary photons in the state Eq. (5.14). The protocol that we outlined above can be extended to create this state for the N-dimensional protocol. The state now consists of a superposition of $\frac{N}{2}$ modes, so we need $\lceil \log\left(\frac{N}{2}\right)\rceil$ control qubits, one target qubit that is a quantum emitter and $N-1$ optical switches. We require that all modes in the ancillary state that we choose satisfy the following condition:

$$i_0 \neq j_0 \wedge i_1 \neq j_1 \wedge i_{N-2} \neq j_{N-2} \quad \forall \quad |i_0 i_1 \ldots i_{N-2}\rangle, |j_0 j_1 \ldots i_{N-2}\rangle \quad . \tag{5.36}$$

This ensures that we never have to route a photon to the multiple spatial modes and thus we generate photons after each other and apply in total $\frac{N-2}{2}$ delay lines.

6

Comparison of the Protocols

In this thesis, we aimed to generate entangled pairs, and in general herald N-dimensional entanglement, by using higher dimensions to reduce the entangled qubits' memory times. The main problem is performing an efficient Bell state measurement in N dimensions and this has been studied in the context of quantum teleportation. We proposed two protocols that each implement the Bell state measurement and outperform the existing protocols in terms of hardware requirements and average fidelities: the protocol with all input modes from Chapter 4 and the tailored protocol from Chapter 5. In this chapter, we compare how our proposed protocols perform on average fidelity, hardware requirements and success probabilities. We compare our protocols against the permutation protocol from Zhang et al. [48] and a protocol that uses photonic qubits e.g. the two-photon entanglement protocol. We simulate the effect of dephasing and amplitude damping during the generation of multiple qubit pairs with Monte Carlo simulations and we end with recommendations for future research.

6.1. Average Fidelity

In schemes such as the single and two-photon entanglement protocol, the protocol can be executed in parallel in order to generate multiple entangled pairs: the pairs that have been generated successfully are stored during the memory time while the other pairs are being generated. During the memory time, the entangled qubits suffer from dephasing and amplitude damping. To examine the quality of the generated entangled pairs in a more realistic way, we simulate the effects of dephasing and amplitude damping. For more details, see Appendix A.

We simulate the average fidelity for the generation of 2, 3 and 4 and 5 entangled pairs for high-dimensional entanglement protocols versus the two-photon entanglement protocol and we show the results in Figure 6.1 for increasing distances. Since the high-dimensional entanglement protocols entangle the qudit registers with a photonic qudit, they are denoted in the legend as 'qudit'. The two-photon protocol heralds one entangled pair by entangling the qubit register with a photonic qubit and is thus indicated with 'qubit'. We assume that the time of local operations is negligible, for example pulses to generate photon-qudit entanglement as described in Section 4.6. We also assume a dephasing time $T_p = 5$ ms and for amplitude damping we assume a relaxation time of $T_1 = 10$ ms for the memory qubits [35][47]. Note that if the coherence time of the memory qubits becomes very long $T_{\mathrm{coh}} \gg T_{\mathrm{gen}} e^{L/L_{\mathrm{att}}}$ the high-dimensional protocols will not offer a significant advantage. However, this requires coherence times that scale exponentially with distance.

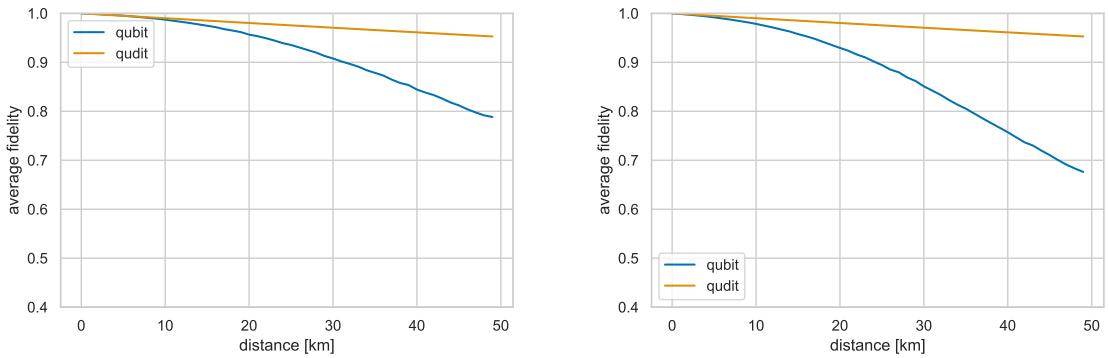

(a) Two generated Bell pairs.

(b) Three generated Bell pairs.

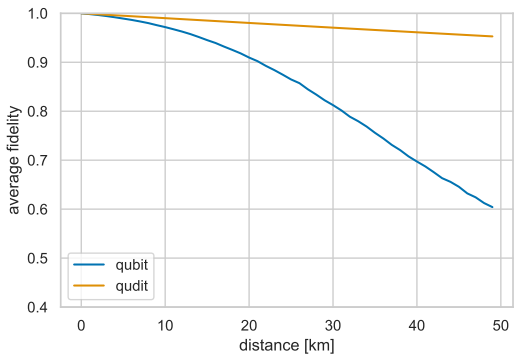

(c) Four generated Bell pairs.

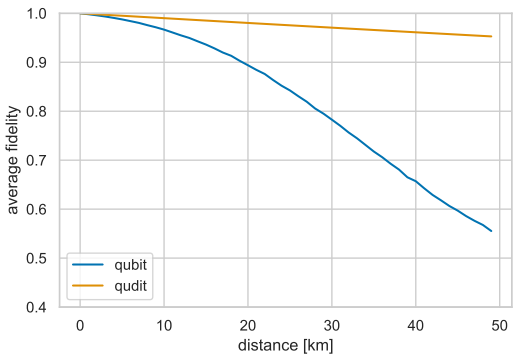

(d) Five generated Bell pairs.

Figure 6.1: Average fidelities for the generation of 2 (a), 3 (b), 4 (c) and 5 (d) entangled qubit pairs versus distance for the two-photon entanglement protocol (indicated with 'qubit') and high-dimensional entanglement protocols ('qudit'). Here we take into account effects of transmission loss of the photons, dephasing and amplitude damping of the qubit register during the generation of all pairs. Note that for large distances, the high-dimensional protocols generate entangled pairs with much higher fidelity than the two-photon protocol.

As the distance increases, the transmission loss increases exponentially according to Eq. (2.9) and thus the expected memory time of the two-photon entanglement protocol increases exponentially. Thus, we expect the fidelity of protocols that use photonic qubits to decrease faster than the average fidelity of qubit pairs heralded with the high-dimensional protocols. In Figure 6.1 we indeed see that high-dimensional protocols always outperform the two-photon entanglement protocol. For increasing distances, the qudit protocols are able to achieve average fidelities that are higher than $F = 0.95$.

6.2. Success Probability

The two-photon entanglement protocol has a success probability of $p_{\text{succ}} = \frac{1}{2}$ and generates one entangled qubit pair. The high-dimensional protocols have various scalings of success probabilities with dimension. In Table 6.1 we give an overview of success probabilities for several dimensions. The values for the permutation protocol are taken from the paper of Zhang et al. They determine their success probabilities in a numerical way for dimensions 3 to 6, thus the success probabilities for dimensions $N = 8$ and $N = 16$ are unknown. The success probabilities for the all-input modes protocol are calculated from Eq. 4.15. Note that this is an upper bound and that there exists no proof that this upper bound is achieved for every dimension. The success probabilities for the tailored protocol are calculated from Eq. (5.21), which we proved to hold for every even dimension in Section 5.3. Since this protocol only heralds entanglement for even dimensions, the odd values do not exist as indicated with $'-'$ in the table below.

dimension N	3	4	5	6	8	16
Luo et al. superposition	≤ 0.22	≤ 0.09	≤ 0.04	≤ 0.02	$\leq 2 \cdot 10^{-3}$	$\leq 1 \cdot 10^{-6}$
permutation p_{tel}	0.11	0.15	0.04	0.06	?	?
permutation p_{tot}	0.22	0.01	0.01	0.001	?	?
tailored	-	0.13	-	0.06	0.03	0.008

Table 6.1: Success probabilities for various dimensions of the high-dimensional entanglement protocols.

The all-input modes protocol performs the worst and the success probability quickly decreases to very low values. The success probabilities of the permutation protocol and the tailored protocol are similar for several dimensions. However to create the superposition of permutation modes, the permutation protocol requires another N-dimensional Bell state measurement. This decreases the total success probability of the permutation protocol and compared to this the tailored protocol vastly outperforms the permutation protocol. The creation of the states that are needed in the tailored protocol is deterministic, so the total success probability is not lowered by this. Even for 16 dimensions, the tailored protocol succeeds in approximately 1% of the attempts and with each successful run heralds $\log_2(16) = 4$ qubits pairs.

6.3. Number of Attempts

The success probabilities of the previous section only take into account if the Bell state measurement succeeds. In practice, the transmission loss of photons reduces the total success probability. To see this effect, we plot the number of attempts to generate two and three entangled pairs against distance in Figure 6.2. Here 'qubit' indicates the two-photon entanglement protocol that is executed twice in parallel. The simultaneous attempt to generate all qubit pairs is counted as one attempt.

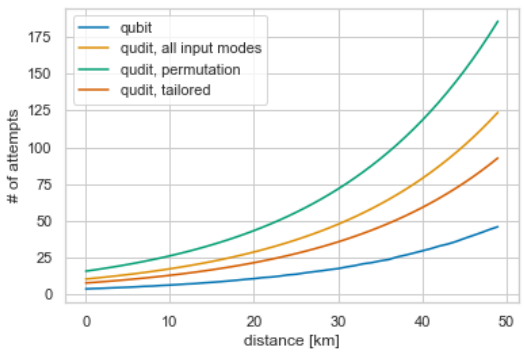

(a) Two generated Bell pairs, so dimension is $N = 2^2 = 4$.

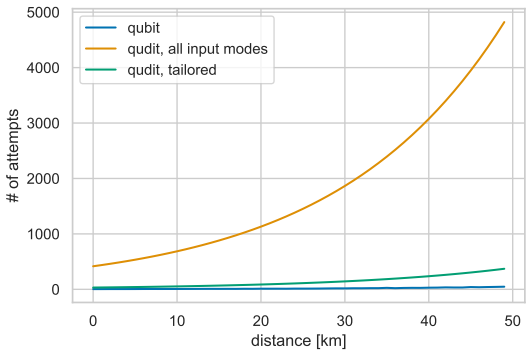

(b) Three generated Bell pairs.

Figure 6.2: Number of attempts before two (a) and three (b) Bell pairs are generated versus distance for the two-photon entanglement protocol (indicated with 'qubit') and various high-dimensional entanglement protocols. Here we take into account transmission loss of the photons.

The probability of successfully transmitting a photon decreases exponentially with distance according to Eq. (2.9). The expected number of attempts thus increases exponentially with distance. We indeed observe this in the figure above. Out of all protocols, the qubit protocols have the largest success probability which lowers their number of attempts. For the high-dimensional entanglement protocols, we use the values from Table 6.1 for dimension $N = 4$ and $N = 8$. For the permutation protocol we have 2 options and we use the total success probability $p_{\text{tot},\,4} = 0.01$. Note that if the permutation state that is necessary for the permutation protocol can be generated in a deterministic way, the success

probability of $p_{\text{tel},\,4} = 0.15$ should be used and in that case the permutation protocol outperforms the tailored protocol with respect to the number of attempts. Also, the success probability of the permutation protocol is not known for $N = 8$, so it is not shown in (b) of Figure 6.2. Since the total success probability would be very low, we would expect it to perform worse than the all-input modes protocol.

6.4. Hardware Requirements

As we describe in Section 6.2, the success probabilities of the all-input modes protocol do not scale well with dimension. The main improvement of this protocol is that the photonic qudits are encoded in time-bins instead of spatial modes, as is done in the protocol of Luo et al. [32]. This yields a quadratic improvement both in the number of spatial modes N required and the number of photon detectors N necessary: from $\mathcal{O}(N^2)$ to $\mathcal{O}(N)$. Also, the encoded state is more robust against bit-flip errors. The time-bin encoding is mainly susceptible to photon loss and since we herald on the measurement of photons this does not affect the fidelity of the entangled pairs.

The implementation of the all-input modes protocol requires one additional energy level available on Bob's side to implement the function from Eq. (4.9). The tailored protocol does not need this additional energy level, but one drawback is that the tailored protocol only works for even dimensions.

The tailored protocol and permutation protocol also use photonic qudits encoded in time-bins, so they yield the same quadratic speedup as the all-input modes protocol and robustness against errors. The preparation of the state required for the permutation protocol, which is a superposition of $N!$ modes, requires a second Bell state measurement. Aside from a lower success probability, this also doubles the number of linear optical elements necessary. The tailored protocol on the other hand requires a much simpler state for the ancillary photons that is a superposition of $\frac{N}{2}$ modes and can be created in a deterministic way as we describe in Section 5.6. For the creation of ancillary modes, $\lceil \log_2(\frac{N}{2}) \rceil + 1$ quantum emitters and $N-2$ optical switches are needed.

6.5. Summary

In this section, we have evaluated the performance of high-dimensional protocols with simulations. We concluded that the high-dimensional entanglement protocols vastly outperform the two-photon entanglement protocol with respect to the average fidelity of multiple generated entangled pairs, especially for large distances. Out of all high-dimensional protocols, the success probabilities of the tailored protocol and the permutation protocol are the highest. However, the success probabilities of the permutation protocol become much lower when the probability to create the permutation state of the ancillary photons is taken into account. Also, the tailored protocol makes use of time-bin encoding and the state of the ancillary photons is easier and deterministic to create than the state required for the permutation protocol.
We conclude that:

- High-dimensional protocols can be used to increase the average fidelity of multiple heralded entangled pairs for distances approximately $L \geq 10$ km.
- Although the tailored protocol only works for even dimensions, it is the only protocol with a polynomial scaling of the total success probability with dimension and an efficient scheme to create the required ancillary state. This gives the best performance on the number of attempts out of all high-dimensional entanglement protocols. Only the two-photon protocol scores better.

7

Conclusions

This research aimed to find protocols that generate entangled pairs and in general herald N-dimensional entanglement between remote nodes with linear optics. By heralding multiple pairs at the same time, we reduce the memory time of the register qudits. From the comparison of the previous chapter, we conclude that for distances $L \geq 10$ km the high-dimensional entanglement protocols vastly outperform the two-photon entanglement protocol that is multiplexed in terms of average fidelities.

By changing the implementation of Luo et al. from spatial mode encodings for the photonic qudits to a time-bin encoding in the all-input modes entanglement protocol, we improved the hardware requirements to $\mathcal{O}(N)$ over $\mathcal{O}(N^2)$ where N is the number of photon detectors or the number of spatial modes. Note that N is also the dimension (number of energy levels) of the qudit register. The time-bin encoding makes the protocol more robust to noise from the environment: it is not susceptible to bit flip errors as other ways of encoding photons are (for example polarization). However, the upper bound of the success probability of the all-input modes protocol decreases exponentially with dimension N: $p_{\text{all-input modes}} \leq \frac{N!}{N^N}$. This makes the all-input modes protocol very difficult to implement in practice.

To circumvent this we propose a novel protocol that scales polynomially with dimension instead of exponentially: the tailored protocol has a success probability of $p_{\text{tailored}} = \frac{2}{N^2}$. This is comparable to the success probabilities of the permutation protocol as proposed by Zhang et al. The main drawback of the permutation protocol is that the ancillary photons need to be in a superposition of all permutation modes. This state is created by another Bell state measurement on entangled qudits. The success probability of this Bell state measurement scales as $\frac{N!}{N^N}$ so the permutation scheme remains very difficult to implement in practice. The ancillary state required for the tailored protocol requires a superposition of $\frac{N}{2}$ modes that can be generated in a deterministic way, which makes it more suitable to implement in practice. The scheme to create the state of the ancillary photons requires $\lceil \log_2(\frac{N}{2}) \rceil + 1$ quantum emitters and $N-2$ optical switches.

7.1. Future Works

In this thesis, we outlined our protocols in a theoretical way, although we did take into account the main sources of errors such as transmission loss, dephasing and amplitude damping. To better understand the effectiveness of the tailored protocol, future works could implement the tailored protocol in practice. An example of such an experiment would be to implement the tailored protocol in 4 dimensions, which would herald two generated qubits pairs at the same time. The theoretical success probability of the Bell state measurement is $p_{\text{tailored, }4} = 0.13$. In practice, there will be other losses that lower the success probability, for example the photon collection efficiency. However, it would be interesting to

look into an implementation with Rydberg atoms. The photon collection efficiency is about 60% [43] and the Rydberg blockade could be used to implement the controlled operations to create the state of the ancillary photons. Other quantum systems could also be considered, for example nitrogen-vacancy centers.

Given that the difference in average fidelity of entangled pairs generated with the single or two-photon protocol versus the tailored protocol becomes larger with distance, future work towards establishing entanglement via satellites with the tailored protocol would also be interesting.

In the N-dimensional tailored protocol, the state of the ancillary photonic qudits is created with $N-1$ optical switches. While optical switches consist of linear optical elements, the phase applied in the switch needs to change abruptly which is arguably not linear. It would be interesting to look into creating the state of the ancillary photons without optical switches.

References

[1] Alain Aspect, Jean Dalibard, and Gérard Roger. “Experimental test of Bell’s inequalities using time-varying analyzers”. In: *Physical review letters* 49.25 (1982), p. 1804.

[2] Xiao-Hui Bao et al. “Quantum teleportation between remote atomic-ensemble quantum memories”. In: *Proceedings of the National Academy of Sciences* 109.50 (2012), pp. 20347–20351.

[3] Ronen Barak and Yacob Ben-Aryeh. “Quantum fast Fourier transform and quantum computation by linear optics”. In: *JOSA B* 24.2 (2007), pp. 231–240.

[4] Sean D Barrett and Pieter Kok. “Efficient high-fidelity quantum computation using matter qubits and linear optics”. In: *Physical Review A* 71.6 (2005), p. 060310.

[5] Helle Bechmann-Pasquinucci and Asher Peres. “Quantum cryptography with 3-state systems”. In: *Physical Review Letters* 85.15 (2000), p. 3313.

[6] Charles H Bennett et al. “Purification of noisy entanglement and faithful teleportation via noisy channels”. In: *Physical review letters* 76.5 (1996), p. 722.

[7] Charles H Bennett et al. “Teleporting an unknown quantum state via dual classical and Einstein-Podolsky-Rosen channels”. In: *Physical review letters* 70.13 (1993), p. 1895.

[8] Hannes Bernien et al. “Heralded entanglement between solid-state qubits separated by three metres”. In: *Nature* 497.7447 (2013), pp. 86–90.

[9] Dik Bouwmeester et al. “Experimental quantum teleportation”. In: *Nature* 390.6660 (1997), pp. 575–579.

[10] Jürgen Brendel et al. “Pulsed energy-time entangled twin-photon source for quantum communication”. In: *Physical Review Letters* 82.12 (1999), p. 2594.

[11] Dagmar BruSS. “Characterizing entanglement”. In: *International Conference on Quantum Information*. Optica Publishing Group. 2001, T4.

[12] John Calsamiglia. “Generalized measurements by linear elements”. In: *Phys. Rev. A* 65 (3 Feb. 2002), p. 030301. DOI: 10.1103/PhysRevA.65.030301. URL: https://link.aps.org/doi/10.1103/PhysRevA.65.030301.

[13] John Calsamiglia and Norbert Lütkenhaus. “Maximum efficiency of a linear-optical Bell-state analyzer”. In: *Applied Physics B* 72 (2001), pp. 67–71.

[14] Nicolas J Cerf et al. “Security of quantum key distribution using d-level systems”. In: *Physical review letters* 88.12 (2002), p. 127902.

[15] Lilian Childress and Ronald Hanson. “Diamond NV centers for quantum computing and quantum networks”. In: *MRS bulletin* 38.2 (2013), pp. 134–138.

[16] David Deutsch et al. “Quantum privacy amplification and the security of quantum cryptography over noisy channels”. In: *Physical review letters* 77.13 (1996), p. 2818.

[17] Miloslav Duek. “Discrimination of the Bell states of qudits by means of linear optics”. In: *Optics communications* 199.1-4 (2001), pp. 161–166.

[18] Artur Ekert and Renato Renner. “The ultimate physical limits of privacy”. In: *Nature* 507.7493 (2014), pp. 443–447.

[19] Manuel Erhard, Mario Krenn, and Anton Zeilinger. “Advances in high-dimensional quantum entanglement”. In: *Nature Reviews Physics* 2.7 (2020), pp. 365–381.

[20] Andrei Faraon et al. “Coupling of nitrogen-vacancy centers to photonic crystal cavities in monocrystalline diamond”. In: *Physical review letters* 109.3 (2012), p. 033604.

[21] Christopher Gerry, Peter Knight, and Peter L Knight. *Introductory quantum optics*. Cambridge university press, 2005.

[22] Daniel Gottesman, Thomas Jennewein, and Sarah Croke. “Longer-baseline telescopes using quantum repeaters”. In: *Physical review letters* 109.7 (2012), p. 070503.

[23] Xueshi Guo et al. “Sensitivity enhancement by mode entanglement in distributed phase sensing”. In: *Quantum Information and Measurement*. Optica Publishing Group. 2019, S4A–4.

[24] Bas Hensen et al. “Loophole-free Bell inequality violation using electron spins separated by 1.3 kilometres”. In: *Nature* 526.7575 (2015), pp. 682–686.

[25] Sophie Hermans et al. “Entangling remote qubits using the single-photon protocol: an in-depth theoretical and experimental study”. In: *New Journal of Physics* (2023).

[26] Chong-Ki Hong, Zhe-Yu Ou, and Leonard Mandel. “Measurement of subpicosecond time intervals between two photons by interference”. In: *Physical review letters* 59.18 (1987), p. 2044.

[27] Yoon-Ho Kim, Sergei P Kulik, and Yanhua Shih. “Quantum teleportation of a polarization state with a complete Bell state measurement”. In: *Physical Review Letters* 86.7 (2001), p. 1370.

[28] H Jeff Kimble. “The quantum internet”. In: *Nature* 453.7198 (2008), pp. 1023–1030.

[29] Emanuel Knill, Raymond Laflamme, and Gerald J Milburn. “A scheme for efficient quantum computation with linear optics”. In: *nature* 409.6816 (2001), pp. 46–52.

[30] Santosh Kumar, Sanjeev Kumar Raghuwanshi, and Ajay Kumar. “Implementation of optical switches using Mach–Zehnder interferometer”. In: *Optical Engineering* 52.9 (2013), pp. 097106–097106.

[31] Dario Lago-Rivera et al. “Telecom-heralded entanglement between multimode solid-state quantum memories”. In: *Nature* 594.7861 (2021), pp. 37–40.

[32] Yi-Han Luo et al. “Quantum teleportation in high dimensions”. In: *Physical review letters* 123.7 (2019), p. 070505.

[33] Norbert Lütkenhaus, John Calsamiglia, and K-A Suominen. “Bell measurements for teleportation”. In: *Physical Review A* 59.5 (1999), p. 3295.

[34] Ivan Marcikic et al. “Long-distance teleportation of qubits at telecommunication wavelengths”. In: *Nature* 421.6922 (2003), pp. 509–513.

[35] CT Nguyen et al. “Quantum network nodes based on diamond qubits with an efficient nanophotonic interface”. In: *Physical review letters* 123.18 (2019), p. 183602.

[36] Michael A Nielsen and Isaac Chuang. *Quantum computation and quantum information*. 2002.

[37] Kazuto Oshima. “More on Quantum Fast Fourier Transform by Linear Optics”. In: *The Open Optics Journal* 8.1 (2014).

[38] Asher Peres and Daniel R Terno. “Quantum information and relativity theory”. In: *Reviews of Modern Physics* 76.1 (2004), p. 93.

[39] Wolfgang Pfaff et al. “Unconditional quantum teleportation between distant solid-state quantum bits”. In: *Science* 345.6196 (2014), pp. 532–535.

[40] Matteo Pompili et al. “Realization of a multinode quantum network of remote solid-state qubits”. In: *Science* 372.6539 (2021), pp. 259–264.

[41] Michael Reck et al. “Experimental realization of any discrete unitary operator”. In: *Physical review letters* 73.1 (1994), p. 58.

[42] Mark Riebe et al. “Deterministic quantum teleportation with atoms”. In: *Nature* 429.6993 (2004), pp. 734–737.

[43] Stephan Ritter et al. “An elementary quantum network of single atoms in optical cavities”. In: *Nature* 484.7393 (2012), pp. 195–200.

[44] Peter W Shor. “Algorithms for quantum computation: discrete logarithms and factoring”. In: *Proceedings 35th annual symposium on foundations of computer science*. Ieee. 1994, pp. 124–134.

[45] Lars Steffen et al. “Deterministic quantum teleportation with feed-forward in a solid state system”. In: *Nature* 500.7462 (2013), pp. 319–322.

[46] Robert Stockill et al. “Phase-tuned entangled state generation between distant spin qubits”. In: *Physical review letters* 119.1 (2017), p. 010503.

[47] Tim Hugo Taminiau et al. “Universal control and error correction in multi-qubit spin registers in diamond”. In: *Nature nanotechnology* 9.3 (2014), pp. 171–176.

[48] Chenyu Zhang et al. “Quantum teleportation of photonic qudits using linear optics”. In: *Physical Review A* 100.3 (2019), p. 032330.

[49] Qiang Zhang et al. “Experimental quantum teleportation of a two-qubit composite system”. In: *Nature Physics* 2.10 (2006), pp. 678–682.

[50] Yunzhe Zheng, Hemant Sharma, and Johannes Borregaard. “Entanglement distribution with minimal memory requirements using time-bin photonic qudits”. In: *PRX Quantum* 3.4 (2022), p. 040319.

A

Decoherence of the Qubit Register

We model the decoherence of the qubit register during waiting time t as a dephasing channel and an amplitude damping channel. We use Krauss operators A_0 and A_1 for dephasing:

$$\begin{aligned} A_0 &= \begin{bmatrix} \sqrt{\frac{1+e^{-t/T_P}}{2}} & 0 \\ 0 & \sqrt{\frac{1+e^{-t/T_P}}{2}} \end{bmatrix} \\ A_1 &= \begin{bmatrix} \sqrt{\frac{1-e^{-t/T_P}}{2}} & 0 \\ 0 & -\sqrt{\frac{1-e^{-t/T_P}}{2}} \end{bmatrix} \end{aligned} \tag{A.1}$$

For the amplitude damping channel we use the Krauss operators are E_0 and E_1:

$$\begin{aligned} E_0 &= \begin{bmatrix} 1 & 0 \\ 0 & e^{-t/2T_1} \end{bmatrix} \\ E_1 &= \begin{bmatrix} 0 & \sqrt{1-e^{-t/T_1}} \\ 0 & 0 \end{bmatrix} \end{aligned} \tag{A.2}$$

We model the decoherence of ρ as:

$$\tilde{\rho} = \sum_{i=0,1;j=0,1} (A_i E_j)\rho(A_i E_j)^\dagger \tag{A.3}$$

We assume a dephasing time of $T_p = 5$ ms and for amplitude damping we assume a relaxation time of $T_1 = 10$ ms for the memory qubits [35][47]. For the high-dimensional entanglement protocols, the waiting time is equal to the time it takes to run the protocol once: $t = \frac{L}{c}$. For the single photon protocol we simulate the waiting time with a Monte Carlo simulation that averages over 10000 repetitions.